Development of DNA Aptamers against *Plasmodium falciparum* Blood Stages Using Cell-SELEX

Elena Lantero[1,2,3], Alexandros Belavilas-Trovas[1,2,3], Arnau Biosca[1,2,3], Paula Recolons[1,2,3], Ernest Moles[4,5,6], Elena Sulleiro[7], Francesc Zarzuela[7], Yunuen Ávalos-Padilla[1,2,3], Miriam Ramírez[2], Xavier Fernàndez-Busquets[1,2,3*]

[1] Nanomalaria Group, Institute for Bioengineering of Catalonia (IBEC), The Barcelona Institute of Science and Technology, Baldiri Reixac 10-12, ES-08028 Barcelona, Spain
[2] Barcelona Institute for Global Health (ISGlobal, Hospital Clínic-Universitat de Barcelona), Rosselló 149-153, ES-08036 Barcelona, Spain
[3] Nanoscience and Nanotechnology Institute (IN2UB), University of Barcelona, Martí i Franquès 1, ES-08028 Barcelona, Spain
[4] Children's Cancer Institute, Lowy Cancer Research Centre, UNSW Sydney, Randwick, NSW, Australia
[5] School of Women's and Children's Health, UNSW Sydney, Sydney, NSW, Australia
[6] ARC Centre of Excellence in Convergent Bio-Nano Science and Technology, Australian Centre for NanoMedicine, UNSW Sydney, Sydney, Australia
[7] Microbiology Department, Vall d'Hebron University Hospital (VHUH), Universitat Autònoma de Barcelona, Barcelona, Spain
*** Corresponding author: Tel.: +34 93 227 5400 (ext 4581); Fax: +34 93 312 9410;**
E-mail addresses: xfernandez_busquets@ub.edu (Xavier Fernàndez-Busquets)
Submitted date (March 09, 2020)
Accepted date (April 22, 2020)

Abstract

New biomarkers have to be developed in order to increase the performance of current antigen-based malaria rapid diagnosis. Antibody production often involves the use of laboratory animals and is time-consuming and costly, especially when the target is *Plasmodium*, whose variable antigen expression complicates the development of long-lived biomarkers. To circumvent these obstacles, we have applied the Systematic Evolution of Ligands by EXponential enrichment method to the rapid identification of

DNA aptamers against *Plasmodium falciparum*-infected red blood cells (pRBCs). Five 70 b-long ssDNA sequences, and their shorter forms without the flanking PCR primer-binding regions, have been identified having a highly specific binding of pRBCs versus non-infected erythrocytes. Structural analysis revealed G-enriched sequences compatible with the formation of G-quadruplexes. The selected aptamers recognized intracellular epitopes with apparent K_ds in the μM range in both fixed and non-fixed saponin-permeabilized pRBCs, improving >30-fold the pRBC detection in comparison with aptamers raised against *Plasmodium* lactate dehydrogenase, the gold standard antigen for current malaria diagnostic tests. In thin blood smears of clinical samples the aptamers reported in this work specifically bound all *P. falciparum* stages vs. non-infected erythrocytes, and also detected early and late stages of the human malaria parasites *Plasmodium vivax, Plasmodium ovale* and *Plasmodium malariae*. The results are discussed in the context of their potential application in future malaria diagnostic devices.

Keywords: Nanomedicine, Malaria, *Plasmodium*, Aptamers, Cell-SELEX

1. INTRODUCTION

Malaria, a parasitic disease caused by different species of *Plasmodium*, is one of the main causes of mortality in the tropical and subtropical world population. Although five species cause illness in humans, the most virulent and fatal is *Plasmodium falciparum,* especially when the infection occurs in young children and pregnant women [1]. The World Health Organization (WHO) Global Technical Strategy for

Malaria 2016-2030 lists the universal access to malaria diagnosis as an essential part of the strategic framework that should eventually lead to eradicating the disease [2], since knowing parasitemia and parasite species is crucial in order to select the most appropriate drug treatment. Currently, national malaria programs rely on light microscopy and rapid diagnostic tests (RDTs), which are not sensitive enough to detect low parasite density infections (sub-microscopic malaria in which patients are usually asymptomatic) that are key in the transmission dynamics. On the other hand, molecular techniques can detect sub-microscopic malaria, but are inadequate for massive use because of elevated costs or need for highly trained staff. Therefore, new diagnostic methods are needed if the objective is to advance towards malaria eradication [3,4].

Although the parasite synthesizes a vast array of molecules to remodel its host red blood cell (RBC), those exported to the cell surface undergo rapid antigenic variation [5,6]. This fast turnover of exposed antigens counsels a constant search for new therapeutic agents and diagnosis targets. Most current strategies for the identification of specific molecular tags in the malaria parasite or in *Plasmodium*-infected RBCs (pRBCs) rely on a detailed knowledge of the pathogen's physiology and of the pRBC biochemistry or the use of time-consuming and expensive immunological methods such as antibody generation. Alternatively, binding specificities and affinities comparable to those of monoclonal antibodies can be obtained with aptamers, short single-stranded (ss) oligonucleotides capable of specific ligand recognition, much faster and cheaper to produce without having to resort to the

use of laboratory animals [7]. They can be either ssDNA or ssRNA, whose three-dimensional structures formed by their self-folding generates topological features that can specifically recognize molecular regions in a similar way as antibodies bind antigenic determinants. Aptamers are able to distinguish different protein isoforms [8], conformational isomers of the same molecule [9], and common structural epitopes in different proteins like those found in amyloid fibrils [10]. In most cases, aptamer binding to its target inhibits biological activity, e.g. due to interference with the catalytic site of an enzyme or with sites involved in ligand-receptor recognition, or to allosteric effects, such as changes in conformational states resulting in loss of function. Aptamers can be identified by *in vitro* selection against almost any target, including antigens which do not induce immune responses in host animals for antibody production, and small molecules like drugs and even metal ions [11]. The versatility of aptamers to recognize nearly any biomolecule in a very specific manner and their higher dry-storage and lyophilisation stability than antibodies makes them effective as diagnostic tools (aptasensors) [12] and attractive as potential therapeutics [13]. Nucleic acid aptamers, which are typically selected from extremely large libraries (containing $\geq 10^{13}$ different oligonucleotide sequences), can modulate the function of virtually any target of biological interest, making them a preferred method of choice for the identification of new bioactive ligands. For *in vivo* applications, aptamers can be chemically modified to confer them resistance against nucleases or tagged with fluorescent reporters and nanoparticles for subcellular localization and pull-down of target proteins [14], respectively.

Aptamers can be developed by Systematic Evolution of Ligands by EXponential enrichment (SELEX) [15-18], which uses iterative *in vitro* selection of combinatorial RNA or DNA pools against a molecular target for the identification of high-affinity oligonucleotide ligands. The method starts by exposing the molecule of interest to a randomly generated ssDNA or RNA library, retrieving the aptamer/target complexes. The binding oligonucleotides are subsequently amplified in a thermal cycler and the resulting PCR products are dissociated in their complementary single strands, which enter again an affinity selection cycle. This process is repeated as many times as it takes to obtain a pool of oligonucleotides specifically binding the selected target. SELEX has been successfully used to obtain aptamers for diagnostic use in infectious diseases [19,20]. The development of DNA aptamers against *Plasmodium* proteins has been mostly focused on the design of new devices for malaria diagnosis by targeting the parasite's lactate dehydrogenase (LDH) [21-25]. RNA ligands against recombinant *P. falciparum* erythrocyte membrane protein 1 (PfEMP1) have been shown to disrupt aggregates of pRBCs with non-infected erythrocytes (rosettes) that contribute to the pathology of severe malaria by clogging the microvasculature [26]. An attempt to develop therapeutic antimalarial aptamers selected DNA sequences binding the heme group released from hemoglobin as the protein is used as food source by the intraerythrocytic parasite; the resulting suppression of the heme detoxification pathway inhibited *Plasmodium* growth *in vitro* [27].

The variant called cell-SELEX [28-30] uses as targets whole cells or cell membranes [31], and it can be a powerful tool in the discovery of new ligands, as

there is no need for prior knowledge of antigenic features. Using whole cells as targets, aptamers can be selected to bind biomarkers differing between two given cell types or between healthy and diseased cells [28,32]. The capacity of this method for the isolation of high-affinity oligonucleotides against such a complex target as the RBC membrane has been reported [31]. Cell-SELEX offers promising perspectives for the selection of aptamers targeting parasite-derived surface proteins, e.g. in *Trypanosoma* and *Plasmodium* [33,34]. Its full potential as tool for cell surface target discovery has not been deeply probed yet, but the application of aptamer technology has been proposed for the implementation of new adjunct therapies to be used in current malaria treatments [26,35]. Presence of surface proteins related to adhesion and sequestration of parasites is widely known [36], although these are easily lost in the cultured lines of *P. falciparum* without any selection pressure. The high variability in these proteins, a mechanism evolved by the pathogen to escape immune system surveillance [37], increases the difficulty of ligand molecule selection.

In this work we present our results on the development of DNA aptamers against pRBCs infected by *P. falciparum*, with the objective of establishing a method for the rapid identification of new markers for malaria diagnosis that could be also of use in future vaccination or targeted therapeutic strategies.

2. EXPERIMENTS

2.1. Preparation of Target Cells

Unless otherwise indicated, oligonucleotides and other reagents were purchased from Sigma-Aldrich. The *P. falciparum* 3D7 strain was grown *in vitro* in group B human erythrocytes using previously described conditions [38]. Parasites (thawed from glycerol stocks) were cultured at 37 °C in T-25 or T-175 flasks (Thermo Fisher Scientific, Rochester, NY, USA) containing human erythrocytes at 3% hematocrit in Roswell Park Memorial Institute (RPMI) complete medium containing Albumax II (Gibco^{TM}), supplemented with 2 mM L-glutamine, under a gas mixture of 92.5% N_2, 5.5% CO_2, and 2% O_2. RBCs parasitized with late-form trophozoite and schizont parasite stages corresponding to 24-36 h and 36-48 h post-invasion (hpi), respectively, were purified in 70% Percoll (GE Healthcare, Chicago, USA) [39,40]. Parasitemia was determined by microscopic counting of blood smears fixed briefly with methanol and stained for 10 min with Giemsa (Merck Chemicals) diluted 1:10 in Sorenson's buffer, pH 7.2. For culture maintenance, parasitemia was kept below 5% late forms and 10% early forms by dilution with freshly washed RBCs and the medium was changed every 1-2 days. Percoll-purified late stages were pelleted (800× g, 6 min) and subjected to fixation in 4% paraformaldehyde followed by cryopreservation at −80 °C in 44% glycerol, 20 g/l sodium lactate, 230 mg/l KCl, and 12 g/l sodium phosphate, pH 6.8. Non-parasitized RBCs from the same blood batch were also cryopreserved and, when required after thawing, fixed as above for their use in counter-SELEX cycles (see below).

2.2. SELEX Cycles

For the generation of pRBC-specific DNA aptamers using the SELEX technique (Fig. 1), a single-strand nucleic acid library with invariant PCR primer-binding flanking regions on each end and a randomized central sequence of 40 nucleotides (**ATACCAGCTTATTCAATT**NNNNNNNNNNNNNNNNNNNNNNNNNNNNNNNNNNNN**AGATAGTAAGTGCAATCT**, 1 µmol) was purchased from DNA Technology A/S (Denmark). 10 nmol of this DNA library was dissolved in 1 mL of RPMI supplemented with 25 mM HEPES, pH 7.4, 5 mM $MgCl_2$ and 1 mg/mL BSA (binding buffer) and subjected to a first counter-SELEX negative selection process, whereby it was incubated with ca. 10^6 fixed RBCs that had been previously washed three times in washing medium (binding buffer without BSA). Prior to addition to the cells, the library was incubated at 95 °C for 5 min followed by a 10-min incubation in ice. The cells and library mixture was incubated in ice for 1 h under constant stirring (50 rpm), spun down (500× g, 3 min) to remove RBC-binding sequences, and the supernatant containing the free oligonucleotides that did not bind RBCs was added to fixed pRBCs for the next positive selection cycle. This counter-selection step with non-parasitized erythrocytes was repeated again before rounds 4, 7 and 10. After incubation and pull down steps as above, the pelleted cells were rinsed 3 times with washing medium, taken up in 200 µL of double deionized water (ddH_2O; MilliQ system, Millipore) and heated up to 95 °C for 10 min before proceeding to thermal cycler amplification.

pRBC-binding sequences were PCR amplified following the procedures described by Sambrook and Russell [41], using *Taq* DNA polymerase (PCR Master

Mix 2×, Thermo Fisher Scientific). As a rule, 20 cycles were programmed in a DNA 2720 Thermal Cycler (Applied Biosystems) 94 °C/56 °C/72 °C, 30 s each, with a 1-min 94 °C extra incubation before the first cycle. The 5’ ends of forward (5’-ATACCAGCTTATTCAATT-3’) and reverse (5’-AGATTGCACTTACTATCT-3’) primers were derivatized with 6-carboxyfluorescein (6-FAM) and tri-biotin, respectively. The PCR mix was distributed in 30 tubes containing 50 µL of reaction each. The resulting amplification products were precipitated by addition of 0.1 vol of 3 M sodium acetate, pH 5, and 2.5 vol of absolute ethanol, thoroughly mixed, and stored overnight at −20 °C. After centrifugation (20,100× g, 45 min, 4 °C), the DNA pellet was washed with 70% ethanol, spun down for 15 min in the same conditions as above, and dried by solvent evaporation for 35 min in a SpeedVac concentrator (SPD 1010, Savant). Finally, the dry pellet was taken up in washing buffer (30 mM HEPES, 500 mM NaCl, 5 mM EDTA, pH 7).

To purify the forward strand, the PCR-amplified DNA (carrying a tri-biotin tag in the reverse strand) was loaded into a streptavidin column (NeutrAdivin^{TM} High Capacity Agarose Resin, Thermo Fisher Scientific) and placed inside a Micro Bio-Spin chromatography Colum (Bio-Rad). Columns were washed 16 times with washing buffer before DNA addition, and 10 times afterwards. To elute the forward strand (carrying a 6-FAM tag), 400 µL of 0.1 M NaOH were added to the column, which was subsequently vortexed (30 s) and centrifuged (500× g, 30 s). 3 elutions were performed and immediately neutralized with 0.1 vol of 1 M HCl. The eluted ssDNA was precipitated as above and taken up in binding buffer. This

fluorescein-labeled oligonucleotide entered a second identical SELEX cycle and this process was repeated for 10 such rounds of binding and selection, until a set of aptamers was identified that bound pRBCs with the desired specificity and affinity as assessed by fluorescence microscopy and flow cytometry. Finally the selected sequences were subcloned and synthesized in sufficiently large amounts for the characterization of their binding to pRBCs.

2.3. Fluorescence Microscopy and Flow Cytometry Analysis

P. falciparum 3D7 cultures (either fixed, permeabilized non-fixed, or live) and fixed *P. falciparum* NF54 *gexp02-tdTomato* stage IV gametocytes, induced by choline removal [42], and selected by addition of 50 mM N-acetyl-D-glucosamine (choline-sensitive transgenic line kindly provided by Harvie Portugaliza and Alfred Cortés [43]) were incubated in the presence of 120 pmol of oligonucleotides labeled in their 5' ends with 6-FAM (λex/em: 488/525 nm) for 60 min in binding buffer at 4 °C with gentle stirring. Aptamers had been previously pretreated by incubating them for 5 min at 95 °C in washing medium at 10× their final concentration, followed by a 10-min incubation on ice. After rinsing with washing medium, cells were stained for 30 min with 4 µg/mL of the DNA dye Hoechst 33342 (λex/em: 350/461 nm), rinsed with washing medium and placed in a 8-well LabTek chamber slide system (Lab-Tek®II, catalog number 155409). For clinical sample testing, blood was obtained by venous puncture with a syringe and was placed in a tube with 6 mM EDTA as anticoagulant. A drop of blood (3 to 5 µL) was deposited on one end of a microscope slide and gently extended with

another slide. Informed consent was obtained from all blood donors. The preparations were allowed to dry for at least 3 hours before fixing them in methanol:acetone 1:9 prior to incubating with the aptamers. Fluorescence microscopy analysis was done with an Olympus IX51 fluorescence microscope or with a Leica TCS SP5 laser scanning confocal microscope equipped with a DMI6000 inverted microscope, blue diode (405 nm), Argon (458/476/488/496/514 nm), diode pumped solid state (561 nm) and HeNe (594/633 nm) lasers and PLAN APO 63× oil (NA 1.4) immersion objective lens. Non-fixed pRBC cultures were permeabilized with 0.1% w/v saponin in phosphate buffered saline (PBS) for 15 min, rinsed 3 times with washing medium, and treated as above.

For flow cytometry analysis, pRBCs were diluted in PBS to a final concentration of 1-10 × 10^6 cells/mL, and samples were analyzed using a LSRFortessa^{TM} flow cytometer (BD Biosciences) set up with the 5 lasers, 20 parameters standard configuration. The single-cell population was selected on a forward-side scatter scattergram. The fluorochromes Hoechst 33342, 6-FAM, TAMRA or tdTomato, and Alexa Fluor 647 (streptavidin label for detection of biotinylated aptamers) were excited using 350, 488, 561 and 640 nm lasers, and their respective emissions collected with 450/40, 525/40, 582/15 and 730/45 nm filters.

2.4. Subcloning and Sequencing of Candidate Oligonucleotides and 2-D Structure Analysis

After 10 rounds of selection, the enriched oligonucleotide pool was PCR-amplified

using unlabeled forward and reverse primers and *Pfu* DNA polymerase (Biotools). The resulting products were cloned into the pBluescript SK+ plasmid after its linearization with *Sma*I (New England Biolabs) using T4 DNA Ligase (New England Biolabs) and the ligation product was used for the transformation of heat-shock competent TOP10 *Escherichia coli* cells (Thermo Fisher Scientific). The transformed cells were grown overnight at 37 °C in Luria Broth agar plates and the recombinant colonies were differentiated with the blue/white screening method after the induction of *lacZ* expression in the presence of X-gal and IPTG. White clones were randomly chosen from the plates and their plasmids were isolated with the GeneJET Plasmid Miniprep Kit (Thermo Fischer Scientific). The successful insertion of sequences from the original library was validated by PCR with the specific forward and reverse primers and by digestion with the restriction enzymes *Not*I and *Sal*I (New England Biolabs); in both approaches DNA bands with the expected lengths were detected in agarose gels. The positive clones were finally sequenced using T7P universal primers (Sanger sequencing service, GENEWIZ GmbH, Leipzig, Germany; https://www.genewiz.com/en-GB/Public/Services/Sanger-Sequencing).

2-D structure analysis was done using the mfold web server (http://unafold.rna.albany.edu/) [44], completing the DNA folding form and selecting ion and temperature conditions present in our incubations (140 mM Na^+ and 5.4 mM Mg^{2+}, 4 °C). The potential presence of G-quadruplexes was analyzed using the Quadruplex forming G-Rich Sequences (QGRS) Mapper (http://bioinformatics.ramapo.edu/QGRS/index.php) [45], which was applied for

predicting the position and the G-score (likelihood to form a stable G-quadruplex).

2.5. Design of a Random Aptamer to be Used as Negative Control

A negative control aptamer (700) was designed by means of an in-house Python script that printed a random 40-base oligonucleotide with the following relative frequencies: A = 17.5%; T = 55%; C = 10% and G = 17.5%. These selected frequencies were obtained by analyzing the relative base frequency of aptamers 19, 24, 30, 77 and 78 (A = 11.22%, T = 17.85%, C = 16.32% and G = 54.59%), and by substituting the frequency of A for C, T for G, G for T and C for A). Frequencies were rounded to obtain an aptamer with a natural number of bases and the unmodified primer-binding sequences were finally added at both ends, obtaining the following oligomer: **ATACCAGCTTATTCAATT**AGTTGTGGTTGCAACTTTTTATTATTTGTTCGTA TCTTTA**AGATAGTAAGTGCAATCT**.

2.6. Determination of Apparent K_d and B_{max}

1×10^6 fixed *P. falciparum* 3D7 Percoll-purified trophozoites were incubated in the presence of fluorescein-labeled oligonucleotides (10 different dilutions in triplicates, from 4000 to 7.13 nM, in a final volume of 40 µL) for 60 min in binding buffer at 4 °C. After rinsing twice with washing medium, cells were diluted 1:10 in PBS immediately prior to analysis with a LSRFortessa™ flow cytometer set up with the 4 lasers, 18 parameters standard configuration. The single-cell population was selected on a forward-side scatter scattergram. 6-FAM was excited using a blue laser (488 nm),

and its fluorescence collected through a 525/40 nm filter; mean fluorescence intensity was obtained using Flowing Software 2.5.1 (www.btk.fi/cell-imaging; Cell Imaging Core, Turku Centre for Biotechnology, Finland). The equilibrium dissociation constant (K_d) and density of receptors (B_{max}) [46] of the aptamer-cell interaction was obtained by fitting the dependence of intensity of specific binding on the concentration of the aptamers to the equation $Y = B_{max}\ X/(K_d + X)$ [32]. GraphPad Prism 6 (GraphPad Software, San Diego, USA) was used to plot the saturation curve, selecting analysis of binding by non-linear regression fit, considering one site and comparing total and non-specific (aptamer 700 used as reference) binding data.

2.7. Dot Blots and Western Blots

Protein extracts from 8 to 48 hpi parasites were sequentially obtained from a *P. falciparum* 3D7 culture tightly synchronized at ring stages (0 hpi) using a series of sorbitol lysis (7 vol of 5% sorbitol in ddH_2O was added to pelleted cultures and incubated at 37 °C for 7 min, then spun down and washed with washing medium before being placed again in culture conditions) combined with Percoll purification of late stages during the previous week. Briefly, 2 sorbitol lysis were performed 36 hours apart, followed by a Percoll treatment 36 h after the second sorbitol, and then a final sorbitol was used to select ring stage parasites with a 8-h window after Percoll. Immediately after this last synchronization, cell samples were collected every 8 h, pulled down by centrifugation and washed twice with PBS supplemented with 1× Mini Protease Inhibitor Cocktail (cOmplete™, Roche; one tablet in 10.5 mL for 1×

concentration), and then incubated with a 7-fold cell pellet volume of 0.15% saponin in PBS and 1× cOmplete™ at 4 °C for 15 min. Afterwards, samples were centrifuged at 10,000× g for 15 min and the supernatant was recovered (saponin extract fraction). The pellet was further washed 4-5 times, until there was no hemoglobin visible, and then resuspended in 1-fold cell pellet volume of 1% Triton X-100 in PBS supplemented with 1× cOmplete™ and incubated for 30 min at 4 °C. Then samples were centrifuged at 20,000× g for 30 min and the supernatant was recovered (Triton X-100 extract fraction). The remaining pellet was washed 2 times and taken up in 1-fold cell pellet volume of RIPA buffer (150 mM NaCl, 10% glycerol, 2 mM EDTA, 0.5% sodium deoxycholate, 0.2% SDS, 0.1% Triton X-100, 40 mM tris-HCl, pH 7.6) supplemented with 1× cOmplete™. After 15 min incubation, the sample was vortexed for 1 min and sonicated for 30 s, and after a brief incubation (4 °C, 10 min), it was centrifuged (20,000× g, 4 °C, 15 min) and the supernatant was recovered (RIPA buffer extract fraction).

After determining protein concentration using the Pierce™ BCA Protein Assay Kit (Thermo Fisher Scientific) following the manufacturer's indications, cell extracts were diluted to 0.2 µg protein/µL and 2 µL of them were placed on top of a preactivated polyvinylidene difluoride (PVDF) membrane (BioRad). When the dots dried, the membrane was blocked under orbital stirring (50 rpm) at RT for 1 h with 5% (w/v) skim milk in tris-buffered saline (TBS, 150 mM NaCl, 50 mM tris-HCl, pH 7.6) containing 0.05% Tween 20 ($TBSt_{0.05}$), washed again (3×, 5 min) in $TBSt_{0.05}$, and incubated with 600 nM biotin-labeled pretreated aptamer in $TBSt_{0.05}$ containing 0.1%

(w/v) skim milk (1 h, RT). After 3 washes with $TBSt_{0.05}$ for 5 min each, it was incubated with 1.5 µg/mL of streptavidin-Alexa Fluor 647 in $TBSt_{0.05}$ containing 0.1% (w/v) milk powder (30 min, RT). After 3 final washes with $TBSt_{0.05}$ for 5 min each, fluorescence images of the membrane strips were obtained with an ImageQuant™ LAS 4000 CCD camera system (GE Healthcare Life Sciences) using red epi-illumination and a R670 Cy5 filter.

For Western blots, 300 µg protein of RIPA fraction extracts from 40 to 48 hpi were loaded into a single-well 12.5% polyacrylamide gel and run for 45 min at 120 V. Then they were transferred overnight to a preactivated PVDF membrane (BioRad) at 4 °C and 180 V. Membrane strips were washed (2×, 5 min) with TBS and processed as for dot blots but substituting the biotinylated aptamer plus fluorescent streptavidin step by a 1-h incubation with 600 nM 6-FAM-labeled aptamer, and detecting fluorescence with a Y515 filter. As an alternative protocol, electrophoresed extracts were in-gel fixed for 10 min with acetic acid/methanol/H_2O 1:4:5 (v/v/v) and washed (3× H_2O plus 3× washing medium). The gel was then placed in binding buffer to which pretreated fluorescein-labeled aptamers were added at a final concentration of 600 nM, incubated overnight and washed (3×, washing medium) before visualizing the gel in an ImageQuant™ LAS 4000 transilluminator, where the fluorescent bands were excised and processed for liquid chromatography with tandem mass spectrometry (LC-MS/MS) analysis.

2.8. Pull Down Assays

0.2 mg of streptavidin-coated magnetic beads (Dynabeads™ MyOne™ Streptavidin C1, Thermo Fisher Scientific) were washed 3 times by magnetic separation with 5 mM tris-HCl, 1 M NaCl, 0.5 mM EDTA, 5 mM $MgCl_2$, pH 7.5. After that, beads were resuspended in 200 µL of the same buffer containing 200 pmol of the biotinylated aptamers, and incubated for 1 h under rotation. Supernatant was removed and unspecific binding sites were blocked by incubation with 0.1% BSA (w/v) in PBS for 1 h. After 5 washes with PBS containing 0.1% Tween 20 (v/v), aptamer-coated beads were incubated overnight in 200 µL PBS with a Triton X-100 protein extract of a *P. falciparum* late stage culture containing 12 µg protein. Then the beads were washed 10 times in PBS supplemented with 145 mM NaCl. To elute bound material, beads were resuspended with Laemmli buffer (60 mM tris-HCl, 2% SDS (w/v), 10% glycerol (v/v), 5% 2-mercaptoethanol (v/v) and 0.002% bromophenol blue (w/v), pH 6.8) and heated up to 95 °C; the supernatants were recovered, loaded into a 12.5% polyacrylamide gel and run for 45 min at 120 V. After silver staining, gel slabs were cut for LC-MS/MS analysis.

2.9. In-Gel Tryptic Digestion of Proteins and LC-MS/MS Analysis

After cleaning gel slabs with 50 mM NH_4HCO_3, pH 8.0 (cleaning buffer, CB) and acetonitrile (ACN), the proteins were reduced with 20 mM DTT in CB (60 °C, 60 min) and alkylated in the same buffer supplemented with 50 mM iodoacetamide (RT, 30 min). Gel slices were covered in CB containing 0.1 µg trypsin (sequencing grade modified, Promega), and digested for 16 h at 37 °C. Tryptic peptides were extracted

from the gel matrix with 10% formic acid (FA) and ACN washes, and finally dried in a vacuum centrifuge.

The dry peptide mixtures were analyzed by LC-MS/MS in a nanoACQUITY liquid chromatographer (Waters) coupled to a linear trap quadrupole-Orbitrap Velos (Thermo Scientific) mass spectrometer. The tryptic digests were resuspended in 1 % FA solution, and an aliquot (2 µL) was injected for chromatographic separation. Peptides were trapped in a Symmetry C18TM trap column (5 µm; 180 µm by 20 mm; Waters) and separated using a C18 reverse-phase capillary column (75 µm Øi, 25 cm, nanoACQUITY, 1.7 µm BEH column, Waters). The gradient used for the elution of the peptides was 1 to 40 % B in 30 min, followed by a gradient from 40% to 60% B in 5 min (A: 0.1% FA in water; B: 0.1% FA in ACN), with a 250 nl/min flow rate. Eluted peptides were subjected to electrospray ionization in an emitter needle (PicoTipTM, New Objective) with an applied voltage of 2000 V. Peptide masses (m/z 300-1600) were analyzed in a data-dependent mode where a full Scan MS was acquired in the Orbitrap with a resolution of 60,000 FWHM at 400 m/z. Up to the 15^{th} most abundant peptides (minimum intensity of 500 counts) were selected from each MS scan and then fragmented in the linear ion trap using collisionally induced dissociation (38% normalized collision energy) with helium as the collision gas. The scan time settings were: full MS: 250 ms (1 Microscan) and MSN: 120 ms. Generated *.raw data files were collected with Thermo Xcalibur (v.2.2). A database was created by merging all human protein entries present in the Swiss Prot public database (v.7/3/2019) with all entries for *P. falciparum* isolate 3D7 present in the public database Uniprot (v.

12/12/19). A small database with common laboratory protein contaminants was also added and *.raw data files obtained in the LC-MS/MS analyses were used to search with the SequestHT search engine using Thermo Proteome Discoverer (v. 1.4.1.14) against the aforementioned database. Both target and a decoy database were searched to obtain a false discovery rate (FDR), and thus estimate the number of incorrect peptide-spectrum matches that exceeded a given threshold, applying preestablished search parameters (enzyme: trypsin; missed cleavage: 2; fixed modifications: carbamidomethyl of cysteine; variable modificacions: oxidation of methionine; peptide tolerance: 10 ppm and 0.6 Da for MS and MS/MS spectra, respectively). To improve the sensitivity of the database search, the semi-supervised learning machine Percolator was used to discriminate correct from incorrect peptide spectrum matches. Percolator assigns a q-value to each spectrum, which is defined as the minimal FDR at which the identification is deemed correct (0.01, strict; 0.05, relaxed). These q values are estimated using the distribution of scores from decoy database search. The results were exported as Excel files and only proteins identified with at least two high confidence peptides (FDR $\leq$0.01) were considered. Gene Ontology term enrichment analysis of RBC-EV and pRBC-EV proteomes at cellular component, molecular function, and biological process level were performed with Database for Annotation, Visualization and Integrated Discovery (David 6.8) (https://david.ncifcrf.gov/).

2.10. Ethics Statement

The human blood used in this work for *P. falciparum in vitro* cultures was

commercially obtained from the *Banc de Sang i Teixits* (www.bancsang.net). Blood was not specifically collected for this research; the purchased units had been discarded for transfusion, usually because of an excess of blood relative to anticoagulant solution. Prior to their use, blood units underwent the analytical checks specified in the current legislation. Blood clinical samples were obtained previous obtainment of the informed consent of the donors. Before being delivered to us, unit data were anonymized and irreversibly dissociated, and any identification tag or label had been removed in order to guarantee the non-identification of the blood donor. No blood data were or will be supplied, and the studies reported here were performed in accordance with the current Spanish *Ley Orgánica de Protección de Datos* and *Ley de Investigación Biomédica* and under protocols reviewed and approved by the Ethical Committee on Clinical Research from the *Hospital Clínic de Barcelona* (Reg. HCB/2018/1223, January 23, 2019) and by the Ethical Committee on Drug Research from the *Hospital Universitari Vall d'Hebron* (Reg. PR(AG)68/2020, February 28, 2020).

3. RESULTS

3.1. Design of a SELEX Protocol for the Identification of *Plasmodium*-Specific Aptamers

During its initial development for the search of pRBC-specific targets, the SELEX process was expected to present itself with a number of problems whose solutions

might require the re-examination of standard protocols or the need for controls to be done months after the research started. In this scenario, the intrinsic variant expression of *Plasmodium* antigens [47] presented a significant obstacle if different parasite cultures were to be used throughout the selection, since their changing proteins would be a movable target precluding the enrichment of aptamers recognizing a particular epitope. In addition, if *Plasmodium* cultures had to be prepared weeks apart, different blood batches would need to be used; in preliminary assays where blood from different donors was employed, the SELEX protocol ended up with the unwilling selection of aptamers targeted to blood donor-specific RBC surface antigens (Fig. 2). To minimize these risks, we decided to grow a large pRBC batch cultured with erythrocytes from a single donor, fix it with paraformaldehyde, and store it in frozen aliquots in order to preserve a constant antigen collection throughout the protocol. Because the fixation method used does permeabilize the cells, the potential antigens to be identified could be intracellular pRBC molecules.

Fluorescence microscopy and flow cytometry analysis were used to follow the enrichment in 6-FAM-labeled pRBC-binding aptamers after each SELEX cycle (Fig. 3). Fluorescence microscopy images revealed an increase in the pRBC-associated fluorescein signal with each successive SELEX round, although the intensity of fluorescence in the first cycles was very low and is barely appreciated in Fig. 3A, where the microscope settings applied to all the SELEX rounds were those selected for a correct exposure of round 10. The higher sensitivity of flow cytometry, however, revealed an unexpected finding since even the PCR-amplified original aptamer library

exhibited a significant binding to pRBCs relative to uninfected erythrocytes (Fig. 3B). With each cycle, the fluorescence signal associated to pRBCs increased whereas non-parasitized RBCs remained aptamer-free. The SELEX cycles were stopped at round 10, when the observed pRBC-associated fluorescence was not significantly different from that detected in round 9. Because the *P. falciparum* culture used in these fluorescence microscopy and flow cytometry analyses was prepared from a different blood batch and parasite stock, we concluded that the aptamers obtained recognized epitopes that are not exclusive of the original pRBC population used for SELEX selection.

3.2. Identification of Individual pRBC-Specific Aptamers

The fluorescence microscopy and flow cytometry data presented above suggested that SELEX round 10 was enriched in highly specific pRBC-binding aptamers. In consequence, we proceeded to subclone the round 10 oligonucleotide pool in order to obtain plasmids containing individual aptamers. Five such cloned sequences (aptamers 19, 24, 30, 77 and 78) were PCR-amplified using the fluorescein-labeled forward primer, and when added to fixed pRBC/RBC cocultures they exhibited a complete specificity of binding for pRBCs vs. RBCs (Fig. 4).

After sequencing the five selected oligonucleotides, it was observed that the originally randomized central sequence of 40 nucleotides was in these 5 oligomers largely G-enriched (Fig. 5). Among different architectures, several aptamers have been described to adopt the G-quadruplex structure, which consists of planar arrays of

four guanines, each one of them pairing with two neighbors by Hoogsteen bonding [48]. At least four GG pairs in close vicinity on an oligonucleotide sequence are required for G-quadruplex formation, and, according to 2-D structure analysis, this feature is present in all the five pRBC-binding aptamers that had been randomly subcloned from SELEX round 10 (Fig. 5 and Table 1).

According to fluorescence microscopy imaging, the chemically synthesized fluorescein-labeled aptamers of these five selected sequences specifically bound pRBCs vs. RBCs (Fig. 6A) of cell batches different from those used during the SELEX process, indicating that the cellular structures being detected are truly characteristic of *P. falciparum*-infected erythrocytes. The pRBC subcellular distributions of the aptamers were not identical; although cytosolic localization was evident for all of them, the sequences 19, 24 and 30 clearly labeled the host erythrocyte plasma membrane, whereas 77 and 78 colocalized with vesicular structures (Fig. 6B). pRBC vs. RBC specific binding was quantitatively characterized by flow cytometry (Fig. 6C), which confirmed that the five selected aptamers bound ≥84.5% of late-stage pRBCs and ≤0.06% of non-parasitized RBCs (Table 2). Aptamer 30 exhibited the most efficient pRBC recognition, binding 95.2% of late stages. A control aptamer (700), which was randomly synthesized but designed to contain a base composition well differentiated from that of the five selected sequences, bound ca. 19.6% of pRBCs. When 6-FAM was substituted by the reporter group TAMRA, binding specificity decreased significantly for aptamer 30 (Table 2), suggesting an effect on oligonucleotide folding of the fluorescein group present on the aptamer 5'

end during the SELEX cycles.

Gametocytes, the sole *Plasmodium* stage that can be transmitted from the human to the mosquito vector, were occasionally observed to be also targeted by some aptamers (e.g. aptamer 30 in Fig. 6A), which led us to perform a detailed flow cytometry *in vitro* study of *P. falciparum* gametocyte targeting. The results obtained (Table 3) indicate that the selected aptamers bind a significant number of gametocytes, being aptamer 30 the best performing sequence, with >60% of gametocytes detected.

The aptamer 2008s, developed against *P. falciparum* LDH, has been postulated as an ideal biosensor for malaria diagnostic devices [22]. 2008s biotinylated in its 5' end has been used in targeting analysis assays performed with purified LDH or with cell extracts [49,50]. We have compared on fixed cells the targeting performance of biotin-2008s with that of the aptamers described here, all of them 5'-biotinylated (Table 4). The flow cytometry results obtained showed a >30 fold improvement in the detection of pRBCs with any of the five aptamers presented in this work relative to 2008s.

Removal of the PCR primer-binding flanking sequences had different effects on the targeting specificity of the variable 40-base oligonucleotides which were selected (Table 2): whereas for aptamers 30 and 78 the change was small, for the other three sequences their shortened forms exhibited a more pronounced reduction in cell target binding, especially evident for oligonucleotide 19, whose late-stage pRBC affinity dropped from 93.0% to 58.5%. According to flow cytometry data of whole cells, and consistently with the use of late-stage pRBCs for the SELEX cycles, early ring stages

were not bound by any of the selected sequences. However, RIPA buffer extracts of all stages were positive for all five aptamers (see Fig. 7 for aptamer 19; data not shown for the other aptamers), indicating the presence from early rings to mature schizonts of the targeted epitope(s), whose presence dramatically increased along the intraerythrocytic parasite cycle.

3.3. Calculation of Apparent K_d, Apparent B_{max}, and Preliminary Sensitivity Evaluation of *Plasmodium*-Specific Aptamers

The apparent affinity for target cells of the selected fluorescein-labeled aptamers was measured by incubating serial dilutions of them with fixed 3D7 *P. falciparum* trophozoites, using a random sequence as nonspecific binding control (Fig. 8 and Table 5). Upon removal of the flanking PCR primer-binding sequences (to obtain aptamers 19s, 24s, 30s, 77s and 78s) the new apparent K_d for aptamers 24 and 77 did not change significantly (1.14/1.07 and 1.07/0.90, respectively), whereas for oligonucleotides 19, 30 and 78 the shorter forms had a lower affinity for pRBCs (apparent K_d values: 0.46/1.10, 0.61/1.53, and 0.33/1.77, respectively). Although the apparent K_d between different aptamers might be influenced by the concentration of their respective antigens in the cells if the aptamers are targeting different molecules, the disparities between the full-length aptamers and the same sequences after the removal of the primer sequences are expected to be mostly influenced by the change in affinity of the oligonucleotides for their corresponding antigens as the primer-binding regions of their sequences are eliminated.

Four out of the five short aptamers (with exception of 19s) improved in B_{max} relative to the full-length sequences, suggesting that they were able to bind more target sites inside cells, since these shortened sequences likely encounter less steric impediments due to their smaller size. Therefore, a decrease in antigen affinity can be compensated by more available ligands. As a preliminary evaluation of aptamer performance, a ratio can be established between the apparent B_{max} and the apparent K_d (binding potential, BP = B_{max}/K_d). The higher this relation, the better cell labeling by the corresponding oligonucleotide, since it will have either a lower K_d (and higher affinity) or a higher B_{max} (and more binding sites), or both. The aptamer ranking according to BP was 30s > 19 > 78 > 24s > 77s > 30 > 78s > 24 > 77 > 19s. No correlation was observed between the efficacy of aptamer target detection and the presence or absence of the PCR primer-binding sequences.

The changes in K_d, B_{max} and BP for each aptamer upon flanking sequence removal (Table 6) showed that whereas K_d decreased or timidly improved (+7% and +19% for 24/24s and 77/77s, respectively), B_{max} increased significantly for the shorter oligonucleotides except for 19/19s, where it fell by 70%. BP values indicated that when the primer-binding flanking sequences were absent, the overall targeting performance ameliorated for 24/24s and, especially, for 30/30s and 77/77s, but it clearly worsened for 78/78s and still more significantly for 19/19s. These results indicated that eliminating the flanking sequences, which were not selected during the SELEX process, can in some cases result in a loss of aptamer binding affinity for the corresponding cell target.

Targeting assays with non-fixed, saponin-permeabilized cells revealed also a pRBC-specific binding of all 5 aptamers (Fig. 9 and Table 7), indicating that the observed specificity was not derived from a fixation artifact. RBCs burst at the saponin concentration used, and most cellular structures remaining in the sample were *P. falciparum* parasites bounded by their parasitophorous vacuole membrane (PVM), exhibiting characteristic rounded shapes slightly smaller than erythrocytes. RBC plasma membrane remains and other erythrocyte debris were still visible around some PVM-enclosed parasites (e.g. see aptamer 19 panel in Fig. 9B). Since all aptamers stained both the PVM (Fig. 9) and the pRBC plasma membrane (Fig. 6 and cell debris in Fig. 9), the targeted epitope(s) likely correspond to parasite molecules that are exported to both cell membranes. This is in agreement with dot blot data (Fig. 7) indicating the presence of the sought-after antigen(s) in Triton X-100 and, especially, in RIPA buffer extracts, which contain cell membrane-bound components. However, targeting assays with live cells did not show binding of the aptamers to pRBCs (data not shown), which clearly suggested that the location of the epitope(s) being detected is intracellular and that the selected oligonucleotides are not able to cross plasma membranes in intact cells.

Pull-down assays using the aptamers bound to magnetic beads resulted in the detection of several pRBC proteins identified by LC-MS/MS (Table 8). Western blots of late stage *P. falciparum* cultures probed with the fluorescein-labeled selected aptamers revealed for all of them dominant bands around 15 and 30 kDa (Fig. 10A). The aptamer 30s, which had the higher predicted BP (Table 5), provided the strongest

signal. This aptamer was used to directly probe a SDS-PAGE lane loaded with the same sample extract that had been analyzed in the Western blot. The main fluorescent band cluster at ca. 15-kDa (Fig. 10B) could be excised and subjected to LC-MS/MS analysis. Again, several *P. falciparum* proteins were identified (Tables 9-11), being the proteasome subunit beta type the sole protein that was also detected in pull-down assays with biotinylated aptamer 19. This result is however not conclusive and although, taken together, these data strongly suggest that all the selected aptamers recognize a single epitope that might be present in multiple parasite proteins, the efforts done to identify this antigen have been unsuccessful so far.

To assess the potential use for the future development of diagnostic devices of the selected aptamers, these were tested on clinical samples of malaria-infected blood that had been previously characterized by Giemsa staining (data not shown). Despite having been evolved against *in vitro* cultured trophozoite and schizont stages, all aptamers targeted ring-stage *P. falciparum* parasites (aptamer 24 targeting shown in Fig. 11; data not shown for the rest of aptamers), which are the main form present in thin blood smears of malaria patients. Whenever present, late stages were always efficiently targeted. Targeting of early and late blood stages was also observed for *Plasmodium ovale* and *Plasmodium malariae* clinical samples (Fig. 12).

4. DISCUSSION

In 2018, around 228 million cases of malaria occurred worldwide, compared with 251 million in 2010 and 231 million in 2017, and the disease caused an estimated 405,000

deaths. In the same year, approximately US$ 2.7 billion was invested globally in malaria control and elimination efforts by governments of malaria endemic countries and international partners – a reduction from the US$ 3.2 billion that was invested in 2017 [1]. Malaria has enormous social and economic relevance, including a negative impact on short-term learning function, loss of work/study productivity, and diagnosis/treatment costs. Whereas the global fight against malaria has evolved from a "control" to a still difficult to implement "eradication strategy" [51], elimination, on the other hand, is technically feasible but would need mass population screening.

P. falciparum histidine-rich protein II (PfHRP-II) is widely used as target antigen for specific detection of this species of the parasite, although some reports have claimed variable results obtained with PfHRP-II-based RDTs [52,53]. In addition, evidences of mutation and deletion of the PfHRP-II gene counsels caution in the use of this biomarker for falciparum malaria [54,55], which led the WHO to recommend researching alternative targets and methods for detection of *P. falciparum* [56]. In this regard, *Plasmodium* glutamate dehydrogenase (PGDH) and lactate dehydrogenase (PLDH) have received increased attention as specific biomarkers for which aptamers have been developed [49,50,57]. Human-infecting plasmodia produce GDH and LDH, whose blood concentration correlates with parasitemia and decreases along patient therapeutic treatment. All *Plasmodium* species infecting humans produce both enzymes, but these are sufficiently variable to allow species-specific recognition [57,58]. Accordingly, PLDH has been proposed as a biomarker for parasitemia estimation, species identification, and treatment response monitoring

[58,59], and aptamers raised against falciparum PLDH exhibited a K_d around 40 nM [22]. Recently, DNA aptamers have been generated against a conserved recombinant domain of the high mobility group box 1 protein of *P. falciparum*, to be developed as potential sensing elements of RDTs [60]. These aptamers incur the risk of a loss in antigen binding efficacy if the molecular targets mutate or exhibit variant expression. To overcome this problem, we have explored here the use of a cell-SELEX approach, which, in addition to individual proteins, might also produce aptamers targeting (i) molecular landscapes present in several parasite molecules or (ii) non-proteinaceous antigens, such as lipids, nucleic acids or polysaccharides. Using inertial microfluidic SELEX, RNA aptamers that recognized distinct, surface-displayed epitopes on pRBCs with nanomolar affinity had been developed [61]. Moreover, cell-SELEX has also been successfully used to select aptamers with dissociation constants in the nanomolar range against leukemia cells [32,62], human hepatoma cell line Hep62 [63], and non-small cell lung cancer [64]. In our study, the apparent K_d range from 0.46 ±0.08 to 1.77 ±0.15 μM for both full-length and shortened aptamers raised against pRBCs is comparable to values reported for aptamers generated against *Salmonella typhimurium* using a similar whole-cell SELEX approach like that employed here [65]. These relatively high K_ds are characteristic of glycan-containing aptamer targets [66]. However, since the corresponding molecular antigens have not been identified yet, these K_d values had to be calculated against whole cells. To the best of our knowledge, all available K_d values in the nM range reported for PLDH aptamers were obtained with techniques that used the purified enzyme: isothermal

titration calorimetry, electrophoretic mobility shift assay and surface plasmon resonance spectroscopy [22]. When exposed to whole cells *in vitro*, all the aptamers studied here bound *P. falciparum*-infected erythrocytes >30-fold better than the PLDH 2008s aptamer, likely because of a larger number of target epitopes present in each cell.

As opposed to using the purified molecular target, calculation of K_d measuring fluorescence intensity in target cells can be misled as the number of binding sites is unknown. This approach, however, can be adequate in the selection of diagnostic aptamers if these are to be tested with whole cells, where the sensitivity of detection will depend on the K_d of the aptamer but also on the abundance and availability of the corresponding molecular target within the crowded intracellular environment. Preliminary binding affinity assays of our aptamers evolved by whole-cell SELEX ended up with the identification of multiple proteins being targeted. This result was consistent with the abundance in *Plasmodium* of highly aggregative [67] or adhesive proteins [68], which could be carried together with the aptamer-binding element(s). Alternatively, the binding of DNA oligonucleotides to *Plasmodium* components might be based on some widely represented parasite epitope or on unspecific interactions with protein primary or secondary structures. G-quadruplexes, for instance, have twice the negative charge density per unit length compared to DNA double helices, thus representing an excellent arrangement for interactions with e.g. cationic proteins [48].

In agreement with the experimental design used here, our cell-SELEX proof of

concept approach has obtained aptamers against *P. falciparum* late blood stages, mostly trophozoites and schizonts. This might limit diagnostic applications, since a clinical *P. falciparum* infection mainly has early blood stages in the blood circulation. However, according to dot blot assays of *in vitro* cultures and fluorescence microscopy analysis of clinical samples, the selected aptamers target ring stages as well. Late stages can also be found in circulation as result of an apparent reduction or delay in sequestration, usually in high parasitemia *P. falciparum* infections, but occasionally also in asymptomatic cases [69]. These observations encourage the exploration of a potential application of the aptamers developed here as components of future RDT devices, where DNA aptamers could substitute for the antibodies currently used as sensing elements [70]. Among the aptamers developed in this work, 30s would be the most suitable for clinical use given its high BP, although even higher diagnostic specificities could be attained with joint detection strategies where two of the selected aptamers could be used together.

As we are progressing from malaria control to elimination, asymptomatic infections will be increasingly elusive to detect since antibody-based RDTs do not have enough sensitivity [71]. Loop-mediated isothermal amplification assays [72] indicate that it is possible to identify such cases, but it is costly compared to microscopic observation and it is still complicated and challenging to be applied worldwide [73,74]. A diagnosis alternative could be offered by synthetic bioreceptors like aptamers, which have already been raised against both pan- and species-specific PLDH [21,49]. The observation that our aptamers bind also erythrocytes infected by *P.*

malariae and *P. ovale* indicates that their potential applications will be in pan-malaria diagnosis. Several biosensing protocols have been developed employing aptamers against *Plasmodium* LDH, such as colorimetric sensing [24], impedance measurements by electrode functionalization [21] or enzyme capture and colorimetric catalysis [75]. Malaria RDTs based on antibody recognition require a lysis step unless the target antigen is secreted, such as HRP-II, and/or a liquid phase to make the sample move by capillarity [76]. Such platforms providing simple, stable and easy-to-use RDTs can be easily adapted to new *Plasmodium*-specific aptamers like the ones developed here, which would only require a cell permeabilization agent included in the corresponding buffers. This direct detection of parasitized cells is an advantage relative to diagnosis methods relying on antibody detection of parasite antigens, whose decay takes longer than the clearance of parasitemia [77]. The recognition of intracellular epitopes might offer some additional benefits such as less susceptibility to the intense variant expression of *Plasmodium* cell surface-exposed molecular tags [5,6].

5. CONCLUSIONS

In this study, several DNA aptamers have been evolved that in *in vitro* studies discriminate with almost complete specificity naïve red blood cells from erythrocytes infected by *P. falciparum* (<0.1% vs. >90% binding to both cell types, respectively). In clinical samples, these aptamers bind all stages of red blood cells infected by *P. falciparum, P. vivax*, *P. ovale* and *P. malariae* in fixed thin blood smears. This work

provides new synthetic biomarkers that can be easily incorporated in the development of a fast, cost-effective, sensitive and easy to use diagnostic tool, which would be a key asset for future malaria elimination policies.

Disclosure

Patent application: Aptamers for detecting *Plasmodium*-infected red blood cells. Application number: EP20382190.5. Application date: March 13, 2020.

Acknowledgements

This research was funded by grants (i) BIO2014-52872-R and IPANAT, RTI2018-094579-B-I00, *Ministerio de Ciencia, Innovación y Universidades* (MICIU), *Agencia Estatal de Investigación*, Spain, and *Fondo Europeo de Desarrollo Regional*, and (ii) 2017-SGR-908, *Generalitat de Catalunya*, Spain. ISGlobal and IBEC are members of the CERCA Programme, *Generalitat de Catalunya*. This research is part of ISGlobal's Program on the Molecular Mechanisms of Malaria which is partially supported by the *Fundación Ramón Areces*. Y.A.-P. acknowledges financial support provided by the European Commission under Horizon 2020's Marie Skłodowska-Curie Actions COFUND scheme (712754) and by the Severo Ochoa programme of the MICIU [SEV-2014-0425 (2015-2019)], which also supported us through the "*Centro de Excelencia Severo Ochoa 2019-2023*" Program (CEX2018-000806-S). We thank Harvie Portugaliza and Alfred Cortés for the *P. falciparum* NF54 *gexp02-tdTomato* transgenic line. We are indebted to Menelaos

Voulgaris for the graphic design of the SELEX cycle scheme.

References and Notes

1. WHO Global Malaria Programme, **2019**. *World Malaria Report 2019*. Geneva: World Health Organization.

2. World Health Organization, **2015**. *Global Technical Strategy for Malaria 2016-2030*. Geneva: World Health Organization.

3. Kasetsirikul, S., Buranapong, J., Srituravanich, W., Kaewthamasorn, M. and Pimpin, A., **2016**. The development of malaria diagnostic techniques: a review of the approaches with focus on dielectrophoretic and magnetophoretic methods. *Malaria Journal 15*(1), pp.358.

4. Pham, N.M., Karlen, W., Beck, H.P. and Delamarche, E., **2018**. Malaria and the 'last' parasite: how can technology help? *Malaria Journal, 17*(1), pp.260.

5. Craig, A. and Scherf, A., **2001**. Molecules on the surface of the *Plasmodium falciparum* infected erythrocyte and their role in malaria pathogenesis and immune evasion. *Molecular and Biochemical Parasitology, 115*(2), pp.129-143.

6. Tilley, L., Dixon, M.W. and Kirk, K., **2011**. The *Plasmodium falciparum*-infected red blood cell. *International Journal of Biochemistry and Cell Biology, 43*(6), pp.839-842.

7. Ruigrok, V.J.B., Levisson, M., Eppink, M.H.M., Smidt, H. and van der Oost, J., **2011**. Alternative affinity tools: more attractive than antibodies? *Biochemical Journal, 436*(1), pp.1.

8. Wang, M.S., Black, J.C., Knowles, M.K. and Reed, S.M., **2011**. C-reactive protein (CRP) aptamer binds to monomeric but not pentameric form of CRP. *Analytical and Bioanalytical Chemistry, 401*(4), pp.1309-1318.

9. Thirunavukarasu, D. and Shi, H., **2015**. An RNA aptamer specific to Hsp70-ATP

conformation inhibits its ATPase activity independent of Hsp40. *Nucleic Acid Therapeutics, 25*(2), pp.103-112.

10. Mitkevich, O.V., Kochneva-Pervukhova, N.V., Surina, E.R., Benevolensky, S.V., Kushnirov, V.V. and Ter-Avanesyan, M.D., **2012**. DNA aptamers detecting generic amyloid epitopes. *Prion, 6*(4), pp.400-406.

11. Stoltenburg, R., Reinemann, C. and Strehlitz, B., **2007**. SELEX-a (r)evolutionary method to generate high-affinity nucleic acid ligands. *Biomolecular Engineering, 24*, pp.381-403.

12. O'Sullivan, C.K., **2002**. Aptasensors - the future of biosensing? *Analytical and Bioanalytical Chemistry, 372*(1), pp.44-48.

13. Warren, C.L., Mohandas, A., Chaturvedi, I. and Ansari, A.Z., **2009**. Macromolecular Interactions: Aptamers. In: *Encyclopedia of Life Sciences*, John Wiley & Sons, Vol. 29, pp.582-594.

14. Gao, S., Zheng, X., Jiao, B. and Wang, L., **2016**. Post-SELEX optimization of aptamers. *Analytical and Bioanalytical Chemistry, 408*(17), pp.4567-4573.

15. Ellington, A.D. and Szostak, J.W., **1990**. *In vitro* selection of RNA molecules that bind specific ligands. *Nature, 346*, pp.818.

16. Tuerk, C. and Gold, L., **1990**. Systematic evolution of ligands by exponential enrichment: RNA ligands to bacteriophage T4 DNA polymerase. *Science, 249*(4968), pp.505.

17. Abelson, J., **1990**. Directed evolution of nucleic acids by independent replication and selection. *Science, 249*(4968), pp.488-489.

18. Robertson, D.L. and Joyce, G.F., **1990**. Selection *in vitro* of an RNA enzyme that specifically cleaves single-stranded DNA. *Nature, 344*, pp.467.

19. Zimbres, F.M., Tárnok, A., Ulrich, H. and Wrenger, C., **2013**. Aptamers: novel molecules as diagnostic markers in bacterial and viral infections? *BioMed Research International, 2013*, pp.731516.

20. Ospina-Villa, J.D., López-Camarillo, C., Castañón-Sánchez, C.A., Soto-Sánchez, J., Ramírez-Moreno, E. and Marchat, L.A., **2018**. Advances on aptamers against protozoan parasites. *Genes, 9*(12), pp.584.

21. Lee, S., Song, K.M., Jeon, W., Jo, H., Shim, Y.B. and Ban, C., **2012**. A highly sensitive aptasensor towards *Plasmodium* lactate dehydrogenase for the diagnosis of malaria. *Biosensors and Bioelectronics, 35*(1), pp.291-296.

22. Cheung, Y.W., Kwok, J., Law, A.W.L., Watt, R.M., Kotaka, M. and Tanner, J.A., **2013**. Structural basis for discriminatory recognition of *Plasmodium* lactate dehydrogenase by a DNA aptamer. *Proceedings of the National Academy of Sciences of the United States of America, 110*(40), pp.15967-15972.

23. Lee, S., Manjunatha, D.H., Jeon, W. and Ban, C., **2014**. Cationic surfactant-based colorimetric detection of *Plasmodium* lactate dehydrogenase, a biomarker for malaria, using the specific DNA aptamer. *PLOS ONE, 9*(7), pp.e100847.

24. Jeon, W., Lee, S., Manjunatha, D.H. and Ban, C., **2013**. A colorimetric aptasensor for the diagnosis of malaria based on cationic polymers and gold nanoparticles. *Analytical Biochemistry, 439*(1), pp.11-16.

25. Godonoga, M., Lin, T.Y., Oshima, A., Sumitomo, K., Tang, M.S.L., Cheung, Y.W., Kinghorn, A.B., Dirkzwager, R.M., Zhou, C., Kuzuya, A., Tanner, J.A. and Heddle, J.G., **2016**. A DNA aptamer recognising a malaria protein biomarker can function as part of a DNA origami assembly. *Scientific Reports, 6*, pp.21266.

26. Barfod, A., Persson, T. and Lindh, J., **2009**. *In vitro* selection of RNA aptamers against a conserved region of the *Plasmodium falciparum* erythrocyte membrane protein 1. *Parasitology Research, 105*(6), pp.1557-1566.

27. Niles, J.C., deRisi, J.L. and Marletta, M.A., **2009**. Inhibiting *Plasmodium falciparum* growth and heme detoxification pathway using heme-binding DNA aptamers. *Proceedings of the National Academy of Sciences of the United States of America, 106*(32), pp.13266-13271.

28. Lyu, Y., Chen, G., Shangguan, D., Zhang, L., Wan, S., Wu, Y., Zhang, H., Duan, L., Liu, C., You, M., Wang, J. and Tan, W., **2016**. Generating cell targeting aptamers for nanotheranostics using cell-SELEX. *Theranostics, 6*(9), pp.1440-1452.

29. Berezovski, M.V., Lechmann, M., Musheev, M.U., Mak, T.W. and Krylov, S.N.,

2008. Aptamer-facilitated biomarker discovery (AptaBiD). *Journal of the American Chemical Society, 130*(28), pp.9137-9143.

30. Sefah, K., Shangguan, D., Xiong, X., O'Donoghue, M.B. and Tan, W., **2010**. Development of DNA aptamers using cell-SELEX. *Nature Protocols, 5*, pp.1169.

31. Morris, K.N., Jensen, K.B., Julin, C.M., Weil, M. and Gold, L., **1998**. High affinity ligands from in vitro selection: complex targets. *Proceedings of the National Academy of Sciences of the United States of America, 95*(6), pp.2902-2907.

32. Shangguan, D., Li, Y., Tang, Z., Cao, Z.C., Chen, H.W., Mallikaratchy, P., Sefah, K., Yang, C.J. and Tan, W., **2006**. Aptamers evolved from live cells as effective molecular probes for cancer study. *Proceedings of the National Academy of Sciences of the United States of America, 103*(32), pp.11838-11843.

33. Ulrich, H. and Wrenger, C., **2009**. Disease-specific biomarker discovery by aptamers. *Cytometry A, 75A*(9), pp.727-733.

34. Nagarkatti, R., Bist, V., Sun, S., Fortes de Araujo, F., Nakhasi, H.L. and Debrabant, A., **2012**. Development of an aptamer-based concentration method for the detection of *Trypanosoma cruzi* in blood. *PLOS ONE, 7*(8), pp.e43533.

35. Nik Kamarudin, N.A.A., Mohammed, N.A. and Mustaffa, K.M.F., **2017**. Aptamer technology: adjunct therapy for malaria. *Biomedicines, 5*(1), pp.1.

36. Albrecht, L., Angeletti, D., Moll, K., Blomqvist, K., Valentini, D., D'Alexandri, F.L., Maurer, M. and Wahlgren, M., **2014**. B-cell epitopes in NTS-DBL1a of PfEMP1 recognized by human antibodies in rosetting *Plasmodium falciparum*. *PLOS ONE, 9*(12), pp.e113248.

37. Chan, J.A., Fowkes, F.J.I. and Beeson, J.G., **2014**. Surface antigens of *Plasmodium falciparum*-infected erythrocytes as immune targets and malaria vaccine candidates. *Cellular and Molecular Life Sciences, 71*(19), pp.3633-3657.

38. Cranmer, S.L., Magowan, C., Liang, J., Coppel, R.L. and Cooke, B.M., **1997**. An

alternative to serum for cultivation of *Plasmodium falciparum in vitro*. *Transactions of the Royal Society of Tropical Medicine and Hygiene, 91*(3), pp.363-365.

39. Lambros, C. and Vanderberg, J.P., **1979**. Synchronization of *Plasmodium falciparum* erythrocytic stages in culture. *Journal of Parasitology, 65*(3), pp.418-420.

40. Radfar, A., Méndez, D., Moneriz, C., Linares, M., Marín-García, P., Puyet, A., Diez, A. and Bautista, J.M., **2009**. Synchronous culture of *Plasmodium falciparum* at high parasitemia levels. *Nature Protocols, 4*(12), pp.1899-1915.

41. Sambrook, J.F. and Russell, D.W., eds., **2001**. *Molecular Cloning: A Laboratory Manual*. 3rd ed. Cold Spring Harbor Laboratory Press, Cold Spring Harbor, New York.

42. Brancucci, N.M.B., Gerdt, J.P., Wang, C., De Niz M., Philip, N., Adapa, S.R., Zhang, M., Hitz, E., Niederwieser, I., Boltryk, S.D., Laffitte, M.C., Clark, M.A., Grüring, C., Ravel, D., Blancke Soares, A., Demas, A., Bopp, S., Rubio-Ruiz, B., Conejo-Garcia, A., Wirth, D.F., Gendaszewska-Darmach, E., Duraisingh, M.T., Adams, J.H., Voss, T.S., Waters, A.P., Jiang, R.H.Y., Clardy, J. and Marti, M., **2017**. Lysophosphatidylcholine regulates sexual stage differentiation in the human malaria parasite *Plasmodium falciparum*. *Cell, 171*(7), pp.1532-1544.

43. Portugaliza, H.P., Llorà-Batlle, O., Rosanas-Urgell, A. and Cortés, A., **2019**. Reporter lines based on the gexp02 promoter enable early quantification of sexual conversion rates in the malaria parasite *Plasmodium falciparum*. *Scientific Reports, 9*(1), pp.14595.

44. Zuker, M., **2003**. Mfold web server for nucleic acid folding and hybridization prediction. *Nucleic Acids Research, 31*(13), pp.3406-3415.

45. Kikin, O., D'Antonio, L. and Bagga, P.S., **2006**. QGRS Mapper: a web-based server for predicting G-quadruplexes in nucleotide sequences. *Nucleic Acids Research, 34*(Web Server issue), pp.W676-W682.

46. Mintun, M.A., Raichle, M.E., Kilbourn, M.R., Wooten, G.F. and Welch, M.J.,

1984. A quantitative model for the *in vivo* assessment of drug binding sites with positron emission tomography. *Annals of Neurology, 15*(3), pp.217-227.

47. Kyes, S., Horrocks, P. and Newbold, C., **2001**. Antigenic variation at the infected red cell surface in malaria. *Annual Review of Microbiology, 55*, pp.673-707.

48. Gatto, B., Palumbo, M. and Sissi, C., **2009**. Nucleic acid aptamers based on the G-quadruplex structure: therapeutic and diagnostic potential. *Current Medicinal Chemistry, 16*(10), pp.1248-1265.

49. Cheung, Y.W., Dirkzwager, R.M., Wong, W.C., Cardoso, J., D'Arc Neves, C.J. and Tanner, J.A., **2018**. Aptamer-mediated *Plasmodium*-specific diagnosis of malaria. *Biochimie, 145*, pp.131-136.

50. Frith, K.A., Fogel, R., Goldring, J.P.D., Krause, R.G.E., Khati, M., Hoppe, H., Cromhout, M.E., Jiwaji, M. and Limson, J.L., **2018**. Towards development of aptamers that specifically bind to lactate dehydrogenase of *Plasmodium falciparum* through epitopic targeting. *Malaria Journal, 17*(1), pp.191.

51. World Health Organization, **2017**. *Integrating Neglected Tropical Diseases into Global Health and Development. 4th WHO Report on Neglected Tropical Diseases*. Geneva: World Health Organization.

52. Mason, D.P., Kawamoto, F., Lin, K., Laoboonchai, A. and Wongsrichanalai, C., **2002**. A comparison of two rapid field immunochromatographic tests to expert microscopy in the diagnosis of malaria. *Acta Tropica, 82*(1), pp.51-59.

53. Rubio, J.M., Buhigas, I., Subirats, M., Baquero, M., Puente, S. and Benito, A., **2001**. Limited level of accuracy provided by available rapid diagnosis tests for malaria enhances the need for PCR-based reference laboratories. *Journal of Clinical Microbiology, 39*(7), pp.2736-2737.

54. Kumar, N., Pande, V., Bhatt, R.M., Shah, N.K., Mishra, N., Srivastava, B., Valecha, N. and Anvikar, A.R., **2013**. Genetic deletion of HRP2 and HRP3 in Indian *Plasmodium falciparum* population and false negative malaria rapid diagnostic test. *Acta Tropica, 125*(1), pp.119-121.

55. Koita, O.A., Doumbo, O.K., Ouattara, A., Tall, L.K., Konaré, A., Diakité, M., Diallo, M., Sagara, I., Masinde, G.L., Doumbo, S.N., Dolo, A., Tounkara, A.,

Traoré, I. and Krogstad, D.J., **2012**. False-negative rapid diagnostic tests for malaria and deletion of the histidine-rich repeat region of the *hrp2* gene. *American Journal of Tropical Medicine and Hygiene, 86*(2), pp.194-198.

56. World Health Organization, **2017**. *WHO Malaria Policy Advisory Committee Meeting Report*. Geneva: World Health Organization.

57. Singh, N.K., Thungon, P.D., Estrela, P. and Goswami, P., **2019**. Development of an aptamer-based field effect transistor biosensor for quantitative detection of *Plasmodium falciparum* glutamate dehydrogenase in serum samples. *Biosensors and Bioelectronics, 123*, pp.30-35.

58. Piper, R.C., Buchanan, I., Choi, Y.H. and Makler, M.T., **2011**. Opportunities for improving pLDH-based malaria diagnostic tests. *Malaria Journal, 10*, pp.213.

59. Atchade, P.S., Doderer-Lang, C., Chabi, N., Perrotey, S., Abdelrahman, T., Akpovi, C.D., Anani, L., Bigot, A., Sanni, A. and Candolfi, E., **2013**. Is a *Plasmodium* lactate dehydrogenase (pLDH) enzyme-linked immunosorbent (ELISA)-based assay a valid tool for detecting risky malaria blood donations in Africa? *Malaria Journal*, *12*, pp.279.

60. Joseph, D.F., Nakamoto, J.A., Garcia Ruiz, O.A., Peñaranda, K., Sanchez-Castro, A.E., Castillo, P.S. and Milón, P., **2019**. DNA aptamers for the recognition of HMGB1 from *Plasmodium falciparum*. *PLOS ONE, 14*(4), pp.e0211756.

61. Birch, C.M., Hou, H.W., Han, J. and Niles, J.C., **2015**. Identification of malaria parasite-infected red blood cell surface aptamers by inertial microfluidic SELEX (I-SELEX). *Scientific Reports, 5*, pp.11347.

62. Sefah, K., Tang, Z.W., Shangguan, D.H., Chen, H., Lopez-Colon, D., Li, Y., Parekh, P., Martin, J., Meng, L., Phillips, J.A., Kim, Y.M. and Tan, W.H., **2009**. Molecular recognition of acute myeloid leukemia using aptamers. *Leukemia, 23*(2), pp.235-244.

63. Xu, J., Teng, I.T., Zhang, L., Delgado, S., Champanhac, C., Cansiz, S., Wu, C., Shan, H. and Tan, W., **2015**. Molecular recognition of human liver cancer cells using DNA aptamers generated via cell-SELEX. *PLOS ONE, 10*(5), pp.e0125863.

64. Zhao, Z., Xu, L., Shi, X., Tan, W., Fang, X. and Shangguan, D., **2009**. Recognition of subtype non-small cell lung cancer by DNA aptamers selected from living cells. *Analyst, 134*(9), pp.1808-1814.

65. Dwivedi, H.P., Smiley, R.D. and Jaykus, L.A., **2013**. Selection of DNA aptamers for capture and detection of *Salmonella typhimurium* using a whole-cell SELEX approach in conjunction with cell sorting. *Applied Microbiology and Biotechnology, 97*(8), pp.3677-3686.

66. Masud, M.M., Kuwahara, M., Ozaki, H. and Sawai, H., **2004**. Sialyllactose-binding modified DNA aptamer bearing additional functionality by SELEX. *Bioorganic and Medicinal Chemistry, 12*(5), pp.1111-1120.

67. Pallarès, I., de Groot, N.S., Iglesias, V., Sant'Anna, R., Biosca, A., Fernàndez-Busquets, X. and Ventura, S., **2018**. Discovering putative prion-like proteins in *Plasmodium falciparum*: a computational and experimental analysis. *Frontiers in Microbiology, 9*, pp.1737.

68. Martí Coma-Cros, E., Biosca, A., Marques, J., Carol, L., Urbán, P., Berenguer, D., Riera, M.C., Delves, M., Sinden, R.E., Valle-Delgado, J.J., Spanos, L., Siden-Kiamos, I., Pérez, P., Paaijmans, K., Rottmann, M., Manfredi, A., Ferruti, P., Ranucci, E. and Fernàndez-Busquets, X., **2018**. Polyamidoamine nanoparticles for the oral administration of antimalarial drugs. *Pharmaceutics, 10*(4), pp.225.

69. Lwin, K.M., Ashley, E.A., Proux, S., Silamut, K., Nosten, F. and McGready, R., **2008**. Clinically uncomplicated *Plasmodium falciparum* malaria with high schizontaemia: a case report. *Malaria Journal, 7*, pp.57.

70. Ruiz-Vega, G., Arias-Alpízar, K., de la Serna, E., Borgheti-Cardoso, L.N., Sulleiro, E., Molina, I., Fernàndez-Busquets, X., Sánchez-Montalvá, A., Del Campo, F.J. and Baldrich, E., **2019**. Electrochemical POC device for fast malaria quantitative diagnosis in whole blood by using magnetic beads, Poly-HRP and microfluidic paper electrodes. *Biosensors and Bioelectronics, 150*, pp.111925.

71. Berzosa, P., de Lucio, A., Romay-Barja, M., Herrador, Z., González, V., García,

L., Fernández-Martínez, A., Santana-Morales, M., Ncogo, P., Valladares, B., Riloha, M. and Benito, A., **2018**. Comparison of three diagnostic methods (microscopy, RDT, and PCR) for the detection of malaria parasites in representative samples from Equatorial Guinea. *Malaria Journal*, *17*(1), pp.333.

72. Oriero, E.C., Okebe, J., Jacobs, J., Van Geertruyden, J.P., Nwakanma, D. and D'Alessandro, U., **2015**. Diagnostic performance of a novel loop-mediated isothermal amplification (LAMP) assay targeting the apicoplast genome for malaria diagnosis in a field setting in sub-Saharan Africa. *Malaria Journal*, *14*, pp.396.

73. Zelman, B.W., Baral, R., Zarlinda, I., Coutrier, F.N., Sanders, K.C., Cotter, C., Herdiana, H., Greenhouse, B., Shretta, R., Gosling, R.D. and Hsiang, M.S., **2018**. Costs and cost-effectiveness of malaria reactive case detection using loop-mediated isothermal amplification compared to microscopy in the low transmission setting of Aceh Province, Indonesia. *Malaria Journal*, *17*(1), pp.220.

74. Tangpukdee, N., Duangdee, C., Wilairatana, P. and Krudsood, S., **2009**. Malaria diagnosis: a brief review. *Korean Journal of Parasitology*, *47*(2), pp.93-102.

75. Dirkzwager, R.M., Kinghorn, A.B., Richards, J.S. and Tanner, J.A., **2015**. APTEC: aptamer-tethered enzyme capture as a novel rapid diagnostic test for malaria. *Chemical Communications*, *51*(22), pp.4697-4700.

76. World Health Organization, **2018**. *Malaria Rapid Diagnostic Test Performance. Results of WHO Product Testing of Malaria RDTs: Round 8 (2016-2018)*. Geneva: World Health Organization.

77. Mayor, A. and Bassat, Q., **2019**. "Resistance" to diagnostics: a serious biological challenge for malaria control and elimination. *EBioMedicine*, *50*, pp.9-10.

Captions

Fig. 1. Scheme of the SELEX process used in this work to obtain DNA aptamers against late-stage pRBCs.

Fig. 2. Obtention of cell-specific aptamers by SELEX. (A) Non-infected RBC preparation containing cells from different blood donors treated with a 6-FAM-labeled oligonucleotide pool selected in *P. falciparum* cultures grown using blood from one of the donors. (B) Confocal 6-FAM fluorescence microscopy image of the same microscope field.

Fig. 3. Progressive selection of pRBC-binding aptamers along the SELEX cycles. (A) Fluorescence microscopy of *in vitro P. falciparum* cultures treated with 6-FAM-labeled aptamer pools selected after SELEX rounds 3, 6, 9 and 10. For an easier identification of colocalizing pixels, the blue color has been changed to red in the merge images. Merge-1: Hoechst 33342 (nuclei) and 6-FAM (oligonucleotides) channels; merge-2: merge-1 superimposed on phase contrast image. The cells used here belonged to a new fixed cell batch different from that used for the SELEX cycles. The microscope settings applied to all the SELEX rounds were those selected for a correct exposure of round 10. (B) Flow cytometry analysis of the same samples from panel A. a.u.: arbitrary units.

Fig. 4. Fluorescence microscopy analysis of the pRBC vs. non-infected RBC binding specificity of five selected aptamers PCR-amplified from individual clones using 6-FAM-labeled forward primers. The cells used here belonged to a new fixed cell batch different from that used for the SELEX cycles. For an easier identification of colocalizing pixels, the blue color of Hoechst 33342 has been changed to red.

Fig. 5. Sequences of the five oligonucleotides whose PCR amplifications using 6-FAM-labeled forward primers showed pRBC binding specificity vs. non-infected RBCs. The PCR primer-binding sequences are indicated in bold; non-bold sequences correspond to the aptamers 19s, 24s, 30s, 77s and 78s. Shadowed in grey are the bases predicted to form G-quadruplexes.

Fig. 6. pRBC vs. non-infected RBC binding specificity analysis in fixed *P. falciparum* cultures of the chemically synthesized aptamers labeled with 6-FAM at the 5' end. (A,B) Fluorescence microscopy analysis of (A) cellular and (B) subcellular aptamer targeting. The arrowhead indicates a *P. falciparum* gametocyte. (C) Quantitative flow cytometry analysis of aptamer targeting. For each panel, late-stage pRBCs are represented in the upper quadrants and 6-FAM-aptamer-bound cells are located in the right-hand quadrants. The cells used here belonged to a new fixed cell batch different from that used during the SELEX cycles. For an easier identification of colocalizing pixels, the blue color of Hoechst 33342 has been

changed to red.

Fig. 7. Dot-blot test of the presence in *P. falciparum* extracts of the epitope(s) recognized by 6-FAM-labeled aptamer 19. Saponin, Triton X-100, and RIPA buffer extracts were obtained at different hpi from a *P. falciparum in vitro* culture initially synchronized at ring stages. Each dot contains 0.4 µg of protein in 2 µL of PBS 1× cOmplete^{TM} buffer. The controls include 2.4 pmol of biotin-labeled aptamer 19 and 0.4 µg of BSA, both in 2 µL of PBS 1× cOmplete^{TM}, plus the same volume of plain buffer.

Fig. 8. Analysis of the binding affinity to *P. falciparum* 3D7 Percoll-purified trophozoites of the selected 6-FAM-labeled aptamers. (A) Full-length aptamers. (B) Aptamers lacking the flanking PCR primer-binding regions.

Fig. 9. pRBC vs. non-infected RBC binding specificity analysis in non-fixed, saponin-permeabilized *P. falciparum* cultures of the chemically synthesized aptamers labeled with 6-FAM at the 5' end. (A,B) Fluorescence microscopy analysis of (A) cellular and (B) subcellular aptamer targeting. (C) Quantitative flow cytometry analysis of aptamer targeting. The cells used here belonged to a new fixed cell batch different from that used during the SELEX cycles. For an easier identification of colocalizing pixels, the blue color of Hoechst 33342 has been changed to red.

Fig. 10. SDS-PAGE and Western blot analysis of aptamer binding. (A) Western blot of late stage *P. falciparum* cultures probed with the selected 6-FAM-labeled aptamers. Since the band pattern was identical for all aptamers, some of them are not shown. (B) 12.5% SDS-PAGE lane where the same late stage extract was loaded but not blotted; instead, it was directly probed with 6-FAM-labeled aptamer 30s. The three bands indicated were separately excised and subjected to LC-MS/MS analysis.

Fig. 11. Fluorescence microscopy analysis of falciparum malaria clinical samples. Thin blood smears of a *P. falciparum* infection were probed with 6-FAM-labeled aptamer 24. (A) Ring stages. (B) Late blood stage. For an easier identification of colocalizing pixels, the blue color of Hoechst 33342 has been changed to red.

Fig. 12. Fluorescence microscopy analysis of malariae, ovale, and vivax malaria clinical samples. Thin blood smears of *P. malariae*, *P. ovale* and *P. vivax* infections were probed with 6-FAM-labeled aptamers. (A) Ring stages. (B) Late blood stages. For an easier identification of colocalizing pixels, the blue color of Hoechst 33342 has been changed to red.

Table 1. G-scores or likelihood of G-quadruplex presence obtained with the QGRS mapper tool.

Table 2. Percentage of fixed late stage pRBC/non-parasitized RBC binding of the different aptamers determined from flow cytometry data.

Table 3. Percentage of fixed *P. falciparum* gametocyte/non-nucleated cell binding of the different aptamers determined from flow cytometry data.

Table 4. Percentage of fixed late-stage pRBC binding of 5'-biotinylated aptamers determined from flow cytometry data.

Table 5. Apparent K_d, B_{max}, and binding potential (BP = B_{max}/K_d ratio) for the selected aptamers.

Table 6. Variation in K_d, B_{max} and BP for full length vs. flanking region-lacking aptamers.

Table 7. Percentage of saponin-permeabilized, non-fixed pRBC binding of the different 6-FAM-labeled aptamers determined from flow cytometry data.

Table 8. *P. falciparum* proteins identified by LC-MS/MS in a pull-down assay performed with biotinylated aptamer 19.

Table 9. *P. falciparum* proteins identified by LC-MS/MS in the band 1 of Fig. 10.

Table 10. *P. falciparum* proteins identified by LC-MS/MS in the band 2 of Fig. 10.

Table 11. *P. falciparum* proteins identified by LC-MS/MS in the band 3 of Fig. 10.

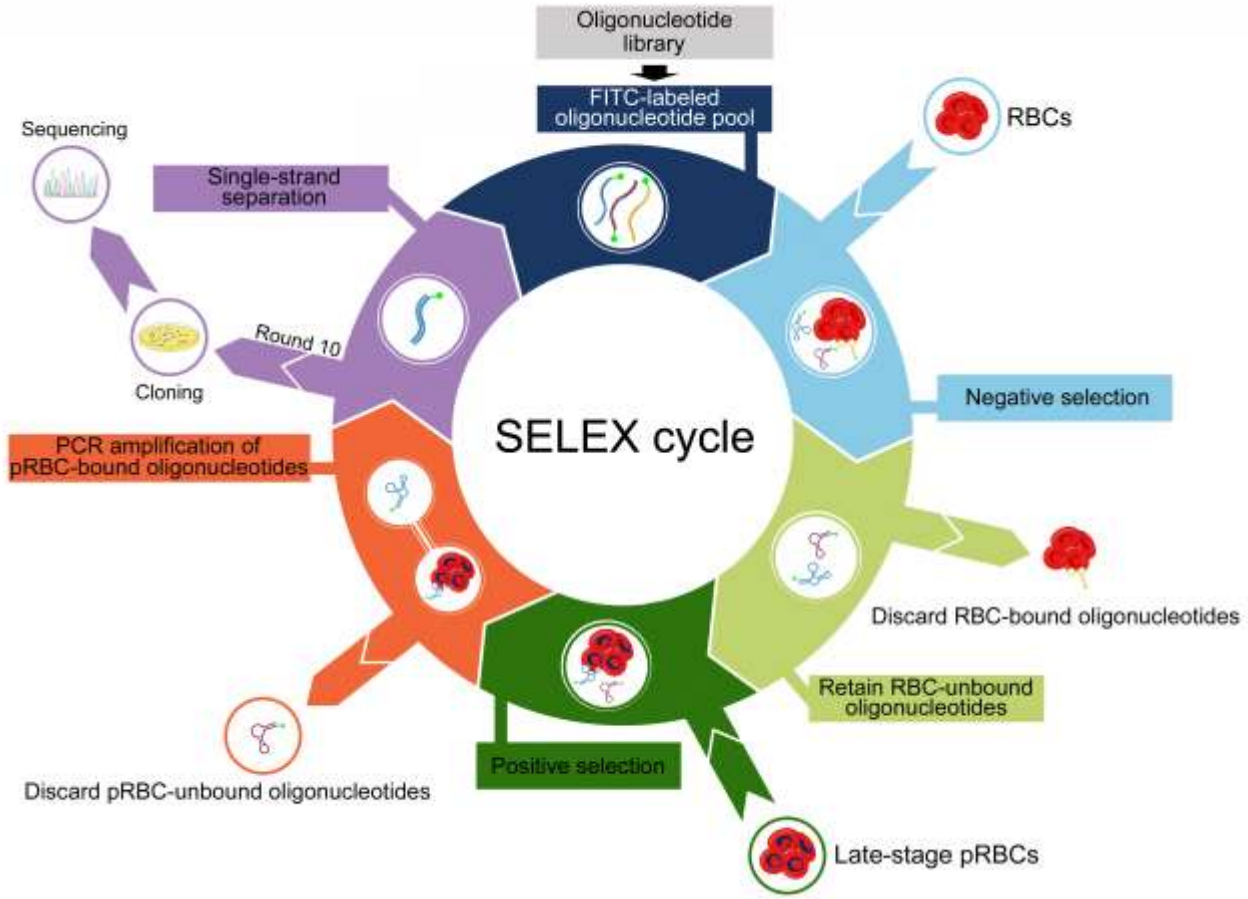

Fig. 1. Scheme of the SELEX process used in this work to obtain DNA aptamers against late-stage pRBCs.

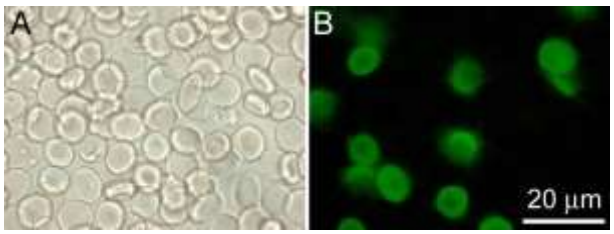

Fig. 2. Obtention of cell-specific aptamers by SELEX. (A) Non-infected RBC preparation containing cells from different blood donors treated with a 6-FAM-labeled oligonucleotide pool selected in *P. falciparum* cultures grown using blood from one of the donors. (B) Confocal 6-FAM fluorescence microscopy image of the same microscope field.

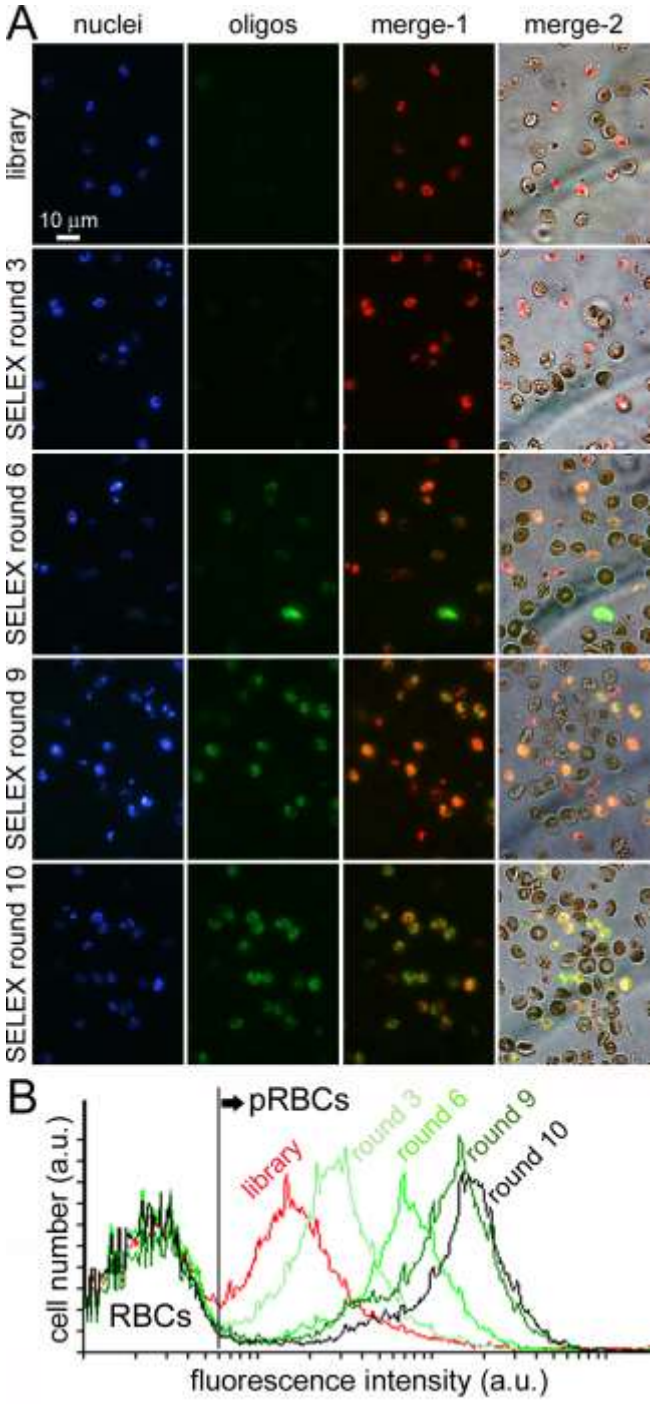

Fig. 3. Progressive selection of pRBC-binding aptamers along the SELEX cycles. (A) Fluorescence microscopy of *in vitro P. falciparum* cultures treated with 6-FAM-labeled aptamer pools selected after SELEX rounds 3, 6, 9 and 10. For an easier identification of colocalizing pixels, the blue color has been changed to red in

the merge images. Merge-1: Hoechst 33342 (nuclei) and 6-FAM (oligonucleotides) channels; merge-2: merge-1 superimposed on phase contrast image. The cells used here belonged to a new fixed cell batch different from that used for the SELEX cycles. The microscope settings applied to all the SELEX rounds were those selected for a correct exposure of round 10. (B) Flow cytometry analysis of the same samples from panel A. a.u.: arbitrary units.

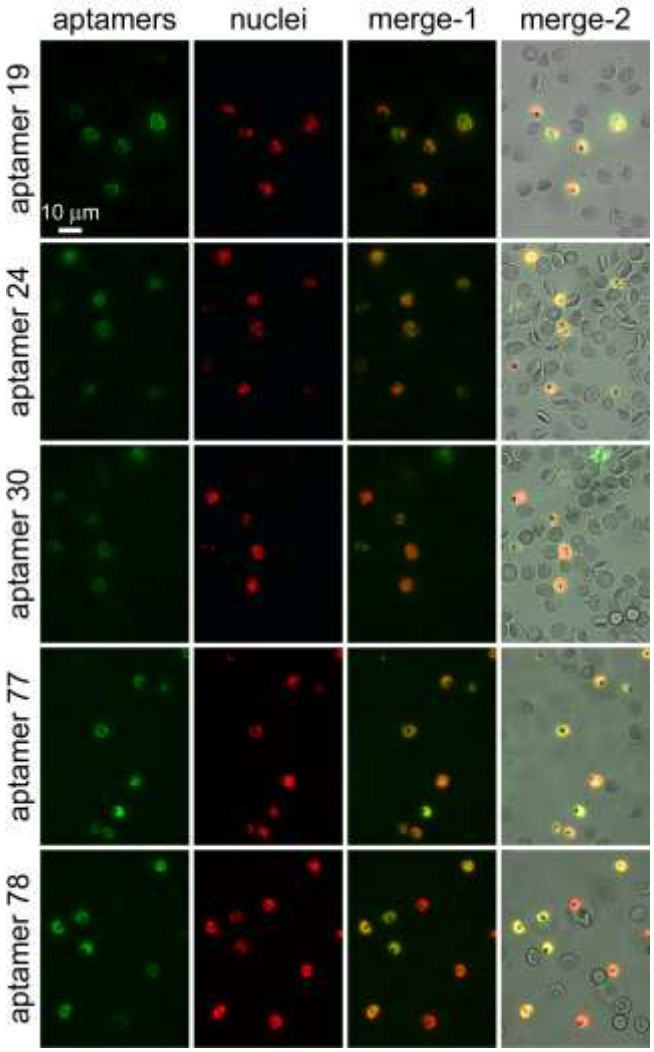

Fig. 4. Fluorescence microscopy analysis of the pRBC vs. non-infected RBC binding specificity of five selected aptamers PCR-amplified from individual clones using 6-FAM-labeled forward primers. The cells used here belonged to a new fixed cell batch different from that used for the SELEX cycles. For an easier identification of colocalizing pixels, the blue color of Hoechst 33342 has been changed to red.

Fig. 5. Sequences of the five oligonucleotides whose PCR amplifications using 6-FAM-labeled forward primers showed pRBC binding specificity vs. non-infected RBCs. The PCR primer-binding sequences are indicated in bold; non-bold sequences correspond to the aptamers 19s, 24s, 30s, 77s and 78s. Shadowed in grey are the bases predicted to form G-quadruplexes.

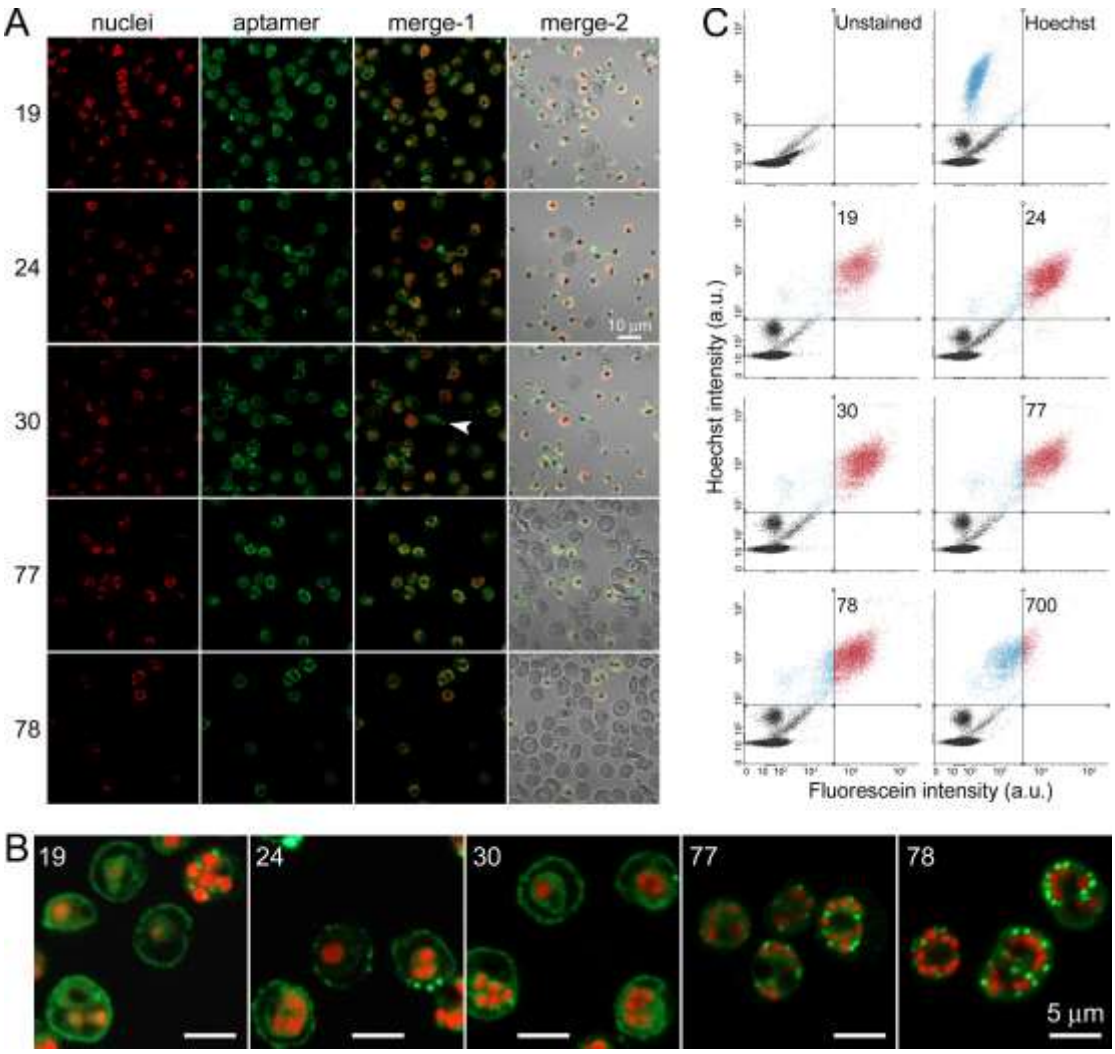

Fig. 6. pRBC vs. non-infected RBC binding specificity analysis in fixed *P. falciparum* cultures of the chemically synthesized aptamers labeled with 6-FAM at the 5' end. (A,B) Fluorescence microscopy analysis of (A) cellular and (B) subcellular aptamer targeting. The arrowhead indicates a *P. falciparum* gametocyte. (C) Quantitative flow cytometry analysis of aptamer targeting. For each panel, late-stage pRBCs are represented in the upper quadrants and 6-FAM-aptamer-bound cells are located in the right-hand quadrants. The cells used here belonged to a new fixed cell batch different from that used during the SELEX cycles. For an easier identification of colocalizing pixels, the blue color of Hoechst 33342 has been changed to red.

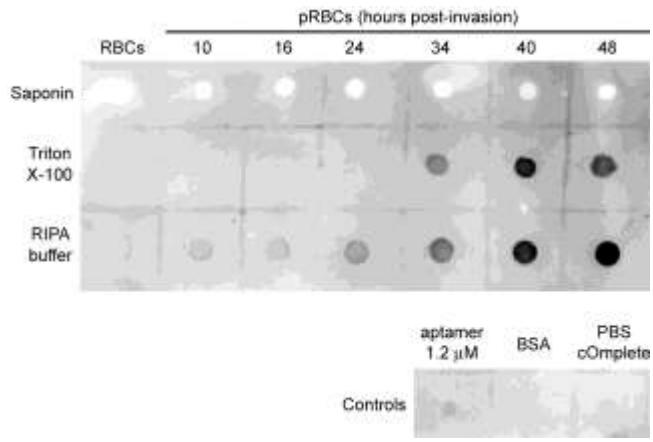

Fig. 7. Dot-blot test of the presence in *P. falciparum* extracts of the epitope(s) recognized by 6-FAM-labeled aptamer 19. Saponin, Triton X-100, and RIPA buffer extracts were obtained at different hpi from a *P. falciparum in vitro* culture initially synchronized at ring stages. Each dot contains 0.4 µg of protein in 2 µL of PBS 1× cOmplete^{TM} buffer. The controls include 2.4 pmol of biotin-labeled aptamer 19 and 0.4 µg of BSA, both in 2 µL of PBS 1× cOmplete^{TM}, plus the same volume of plain buffer.

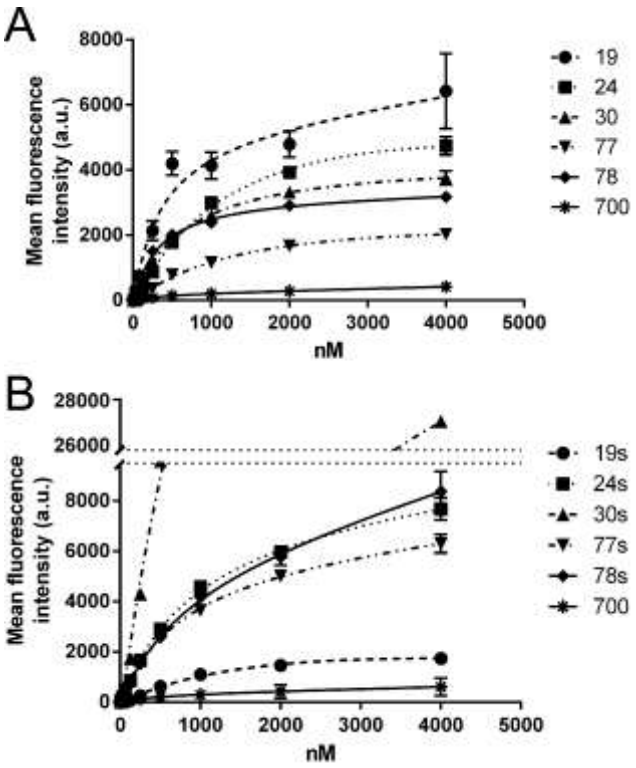

Fig. 8. Analysis of the binding affinity to *P. falciparum* 3D7 Percoll-purified trophozoites of the selected 6-FAM-labeled aptamers. (A) Full-length aptamers. (B) Aptamers lacking the flanking PCR primer-binding regions.

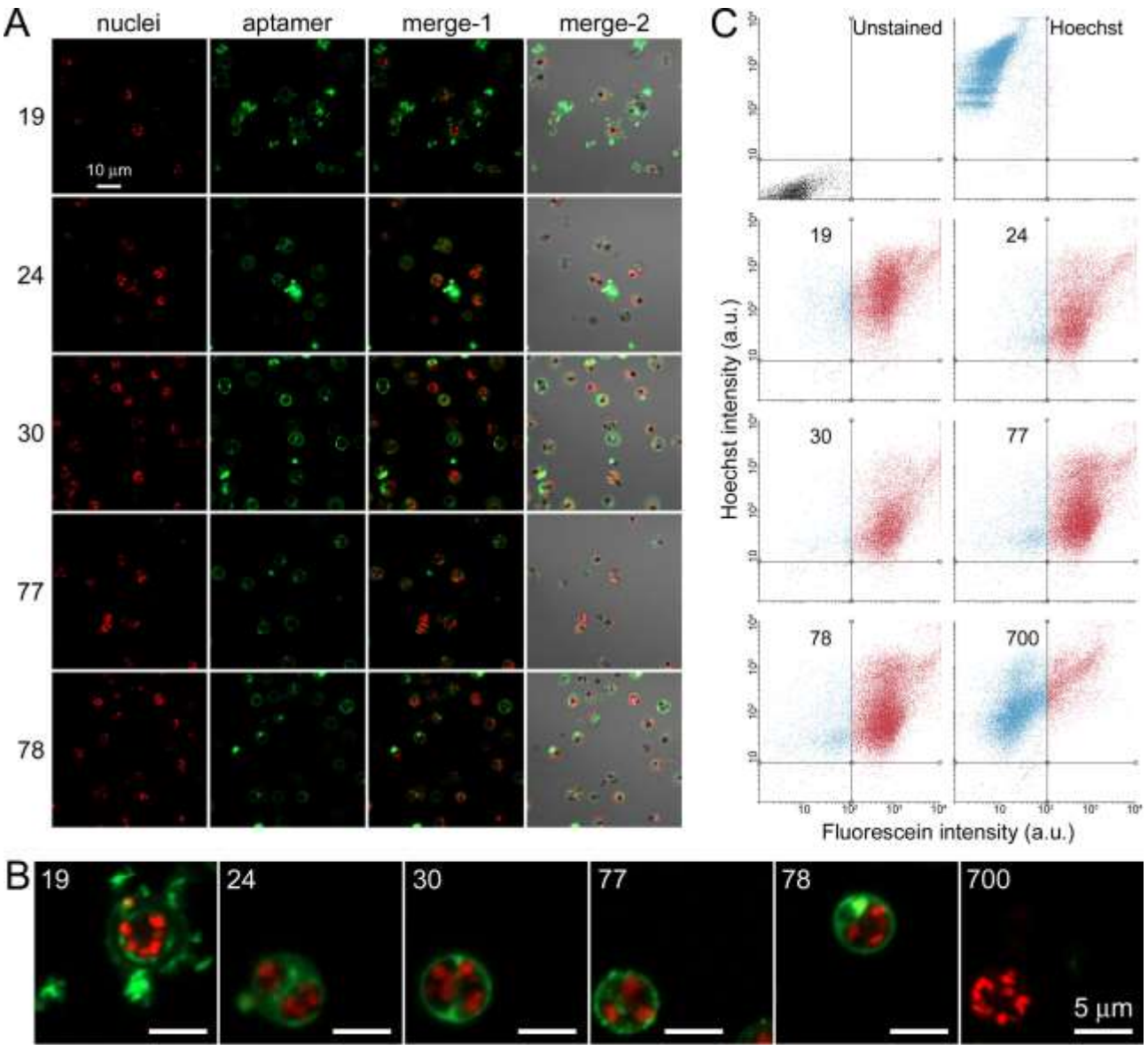

Fig. 9. pRBC vs. non-infected RBC binding specificity analysis in non-fixed, saponin-permeabilized *P. falciparum* cultures of the chemically synthesized aptamers labeled with 6-FAM at the 5' end. (A,B) Fluorescence microscopy analysis of (A) cellular and (B) subcellular aptamer targeting. (C) Quantitative flow cytometry analysis of aptamer targeting. The cells used here belonged to a new fixed cell batch different from that used during the SELEX cycles. For an easier identification of colocalizing pixels, the blue color of Hoechst 33342 has been changed to red.

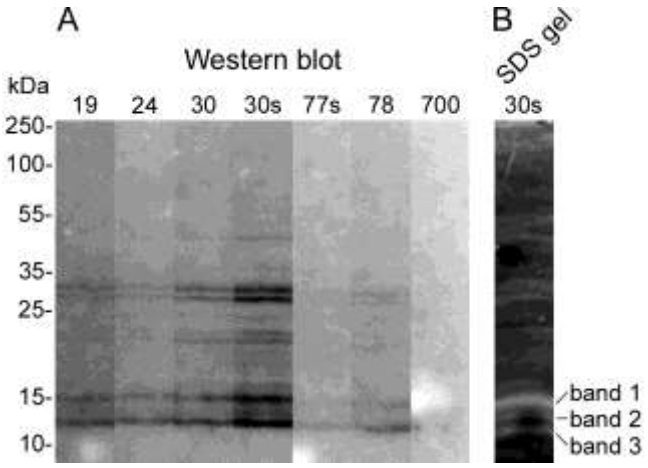

Fig. 10. SDS-PAGE and Western blot analysis of aptamer binding. (A) Western blot of late stage *P. falciparum* cultures probed with the selected 6-FAM-labeled aptamers. Since the band pattern was identical for all aptamers, some of them are not shown. (B) 12.5% SDS-PAGE lane where the same late stage extract was loaded but not blotted; instead, it was directly probed with 6-FAM-labeled aptamer 30s. The three bands indicated were separately excised and subjected to LC-MS/MS analysis.

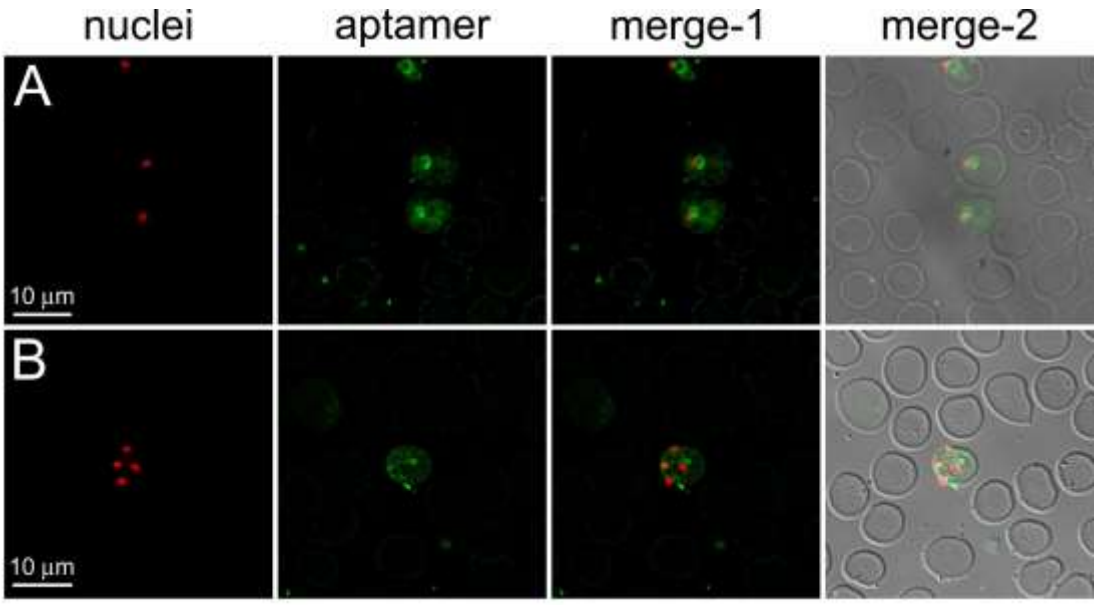

Fig. 11. Fluorescence microscopy analysis of falciparum malaria clinical samples. Thin blood smears of a *P. falciparum* infection were probed with 6-FAM-labeled aptamer 24. (A) Ring stages. (B) Late blood stage. For an easier identification of colocalizing pixels, the blue color of Hoechst 33342 has been changed to red.

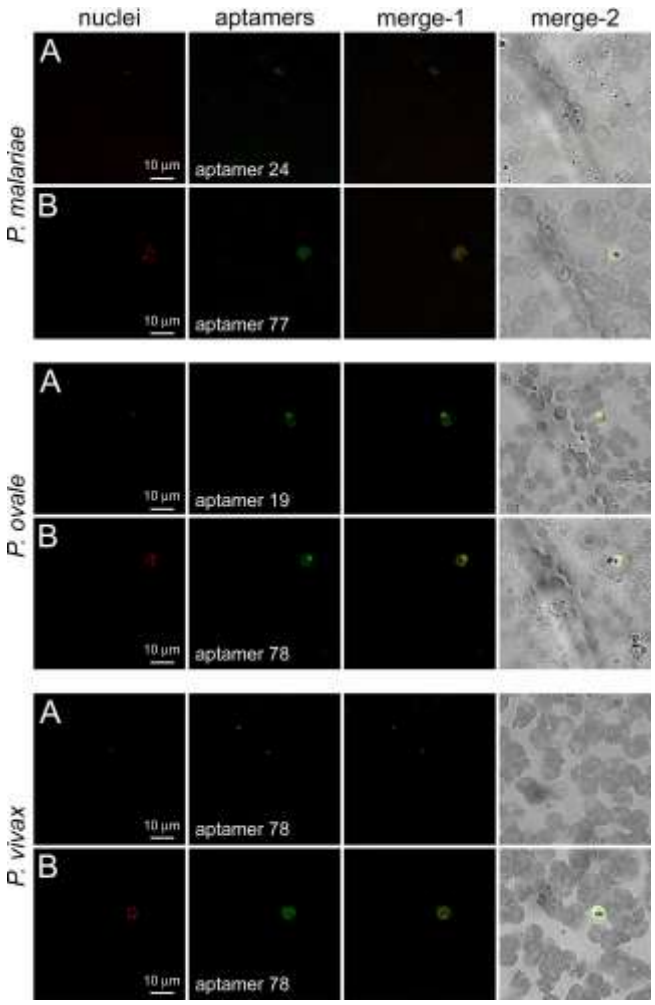

Fig. 12. Fluorescence microscopy analysis of malariae, ovale, and vivax malaria clinical samples. Thin blood smears of *P. malariae*, *P. ovale* and *P. vivax* infections were probed with 6-FAM-labeled aptamers. (A) Ring stages. (B) Late blood stages. For an easier identification of colocalizing pixels, the blue color of Hoechst 33342 has been changed to red.

Table 1. G-scores or likelihood of G-quadruplex presence obtained with the QGRS mapper tool.

Aptamers	*G-score*
19	39
24	41
30	41
77	20, 21*
78	41

* For aptamer 77, two different G-quadruplexes have been predicted.

Table 2. Percentage of fixed late stage pRBC/non-parasitized RBC binding of the different aptamers determined from flow cytometry data.

Aptamer	6-FAM-aptamer (%)	6-FAM-aptamer$_{-\text{flanking sequences}}$ (%)	TAMRA-aptamer (%)
19	93.04/0.02	58.47/0.01	94.39/0.23
24	94.38/0.06	84.16/0.01	94.10/0.07
30	95.16/0.01	96.45/0.01	6.49/0.00
77	88.27/0.00	77.89/0.00	83.73/0.03
78	84.47/0.00	82.79/0.00	87.24/0.05
700	19.60/0.00	not determined	not determined

Table 3. Percentage of fixed *P. falciparum* gametocyte/non-nucleated cell binding of the different aptamers determined from flow cytometry data.

Aptamer	6-FAM-aptamer (%)	6-FAM-aptamer$_{-\text{flanking sequences}}$ (%)
19	61.06/1.22	36.72/0.71
24	59.94/1.15	57.70/1.01
30	59.49/0.88	64.44/3.44
77	not determined	43.94/0.58
78	58.42/0.86	49.04/0.61
700	12.17/0.73	not determined

Table 4. Percentage of fixed late-stage pRBC binding of 5'-biotinylated aptamers determined from flow cytometry data.

	labeled pRBCs (%)
free streptavidin control	0.29
aptamer 19	69.70
aptamer 24	44.47
aptamer 30	50.56
aptamer 77	42.25
aptamer 78	41.19
aptamer 2008s (anti-LDH)	1.24

Table 5. Apparent K_d, B_{max}, and binding potential (BP = B_{max}/K_d ratio) for the selected aptamers.

Aptamer	*Apparent K_d (µM)*	*Apparent B_{max} (a.u.)*	*BP (a.u.·µM^{-1})*
19	0.46 ±0.08	6.18 ±0.36	13.4
24	1.14 ±0.11	5.63 ±0.23	4.9
30	0.61 ±0.04	3.91 ±0.09	6.4
77	1.07 ±0.12	2.06 ±0.10	1.9
78	0.33 ±0.03	3.13 ±0.07	9.4
19s	1.10 ±0.15	1.86 ±0.11	1.7
24s	1.07 ±0.06	8.50 ±0.22	8.0
30s	1.53 ±0.07	36.40 ±0.81	23.8
77s	0.90 ±0.06	6.53 ±0.18	7.3
78s	1.77 ±0.15	10.48 ±0.44	5.9

Table 6. Variation in K_d, B_{max} and BP for full length vs. flanking region-lacking aptamers.

Aptamers	*K_d variation*	*B_{max} variation*	*BP variation*
19/19s	0.42	0.30	0.13
24/24s	1.07	1.51	1.61
30/30s	0.40	9.32	3.70
77/77s	1.19	3.17	3.79
78/78s	0.19	3.35	0.63

Table 7. Percentage of saponin-permeabilized, non-fixed pRBC binding of the different 6-FAM-labeled aptamers determined from flow cytometry data.

Sample	*6-FAM-aptamer-labeled pRBCs (%)*	*6-FAM fluorescence intensity mean (a.u.)*	*6-FAM fluorescence intensity mean increase relative to aptamer 700*
Unstained control	0.0	7.3	–
Hoechst only control	0.5	9.8	–
700	23.4	169.5	1
19	90.6	1191.4	7.0
24	88.4	938.2	5.5
30	93.6	1372.6	8.1
77	78.3	620.7	3.7
78	90.8	893.1	5.3

Table 8. *P. falciparum* proteins identified by LC-MS/MS in a pull-down assay performed with biotinylated aptamer 19.

Accession Number	Protein
Q76NM3	L-lactate dehydrogenase
Q7KQM0	Triosephosphate isomerase
Q8I0P6	Elongation factor 1-alpha
Q8IL80	Thioredoxin peroxidase 1
Q8IE85	60S ribosomal protein L6, putative
Q8IM10	40S ribosomal protein S8
Q8IDV1	60S ribosomal protein L6-2, putative
Q8IJS2	Cytochrome b-c1 complex subunit 7, putative
O96174	Conserved Plasmodium protein
C6KTB1	Protein DJ-1
O77388	HVA22/TB2/DP1 family protein, putative
C0H516	Ras-related protein RAB7
Q8IJ76	Early transcribed membrane protein 10.2
Q8IEM3	60S ribosomal protein L24, putative
Q8I261	Proteasome subunit beta type

Table 9. *P. falciparum* proteins identified by LC-MS/MS in the band 1 of Fig. 10.

Accession Number	Protein
C6KT18	Histone H2A
C6KSV0	Histone H3
Q8I3U6	40S ribosomal protein S11
Q8I502	40S ribosomal protein S17, putative
Q8IBQ5	40S ribosomal protein S10, putative
O00806	60S acidic ribosomal protein P2
O97320	Histone H2A
Q8IIX0	60S acidic ribosomal protein P1, putative
Q8IAX5	40S ribosomal protein S16, putative
Q8IIA2	40S ribosomal protein S18, putative
Q8I3R6	40S ribosomal protein S24
Q8I3J4	Ubiquitin-conjugating enzyme E2 N, putative
O97241	Ubiquitin-conjugating enzyme E2, putative
Q8IC43	Small exported membrane protein 1
Q8IK02	40S ribosomal protein S20e, putative
Q8I463	60S ribosomal protein L31
Q7K6B1	Protein kinase c inhibitor-like protein,putative
Q8IBJ9	Mago nashi protein homologue, putative
Q8IIC4	Ribonucloprotein
C6KT23	60S ribosomal protein L27a, putative
Q8IBV7	Histone H2B
C0H4F3	Bis(5'-nucleosyl)-tetraphosphatase [asymmetrical]
Q8IDP4	Thioredoxin 2
Q8IIV2	Histone H4
Q8IIK8	Peptidyl-prolyl cis-trans isomerase
Q6ZMA7	Sexual stage-specific protein
Q8IIJ4	Uncharacterized protein
Q8I3N5	Pre-mRNA-splicing factor BUD31, putative
Q8IKM6	Inner membrane complex sub-compartment protein 3
C6KSR0	Ubiquitin-conjugating enzyme E2, putative
Q8IDB0	40S ribosomal protein S15
C0H4C7	Uncharacterized protein
Q8IIV1	60S ribosomal protein L36
Q8I713	60S ribosomal protein L28
Q8IHU0	60S ribosomal protein L26, putative
O15770	Glutathione reductase
O97231	60S ribosomal protein L44
Q8ILB7	Mitochondrial import inner membrane translocase subunit TIM17, putative
Q8ID43	Nucleoside diphosphate kinase
Q8IIB9	U6 snRNA-associated Sm-like protein LSm1
Q8IKM5	60S ribosomal protein L27
Q8IDE0	Mitochondrial import inner membrane translocase subunit TIM23, putative
Q8IK04	N-terminal acetyltransferase A complex catalytic subunit ARD1, putative
O97248	40S ribosomal protein S23, putative
O97256	Activator of Hsp90 ATPase, putative
Q8I3B0	60S ribosomal protein L32
Q8I607	Ubiquitin-conjugating enzyme E2
O96258	40S ribosomal protein S26
Q8I6T3	Proteasome subunit beta
Q8IDB8	HVA22-like protein, putative
Q8IAW2	Ubiquitin-conjugating enzyme, putative
Q8IEF9	Ring-exported protein 2
Q8I2G0	Aminopeptidase P
A0A144A2H0	Probable cathepsin C
Q8I573	CHCH domain-containing protein
Q76NN7	Peptidyl-prolyl cis-trans isomerase
Q8IIT3	U6 snRNA-associated Sm-like protein LSm4
C0H4C5	Uncharacterized protein
Q8I5C5	Macrophage migration inhibitory factor
O96217	Ribosomal protein L37
C0H4L5	Replication factor A protein 3, putative
C6S3I6	Succinate dehydrogenase subunit 4, putative
Q8IJU2	60S ribosomal protein L35, putative
Q8IIB4	Cofilin/actin-depolymerizing factor homolog 1
Q8II62	60S ribosomal protein L38
Q8II81	Multiprotein bridging factor type 1, putative
Q8I444	Small ubiquitin-related modifier
Q8I3M0	60S ribosomal protein L23, putative
Q8IE09	40S ribosomal protein S15A, putative
Q8I5Q9	Uncharacterized protein
Q8I306	Transcription elongation factor 1 homolog
C0H4V6	14-3-3 protein

Table 10. *P. falciparum* proteins identified by LC-MS/MS in the band 2 of Fig. 10.

Accession Number	Protein
Q8IIV1	Histone H2B
Q8IBV7	Histone H2B
C6KT18	Histone H2A
O00806	60S acidic ribosomal protein P2
Q8I502	40S ribosomal protein S17, putative
Q8IE09	60S ribosomal protein L23, putative
Q8IJX8	DNA/RNA-binding protein Alba 3
Q8ID43	Nucleoside diphosphate kinase
O77395	40S ribosomal protein S15A, putative
Q8I3U6	40S ribosomal protein S11
Q8IKM6	Inner membrane complex sub-compartment protein 3
Q8IIV2	Histone H4
Q7K6B1	Protein kinase c inhibitor-like protein,putative
Q8I5R8	DNA-directed RNA polymerases I, II, and III subunit RPABC3
Q8IBQ5	40S ribosomal protein S10, putative
Q8I713	60S ribosomal protein L36
Q8IJK8	60S ribosomal protein L30e, putative
Q8I607	Ubiquitin-conjugating enzyme E2
Q8I2G0	Ring-exported protein 2
Q8IAX5	40S ribosomal protein S16, putative
Q8II62	60S ribosomal protein L38
Q8IJ28	Antigen UB05
O97320	Histone H2A
Q8IIT3	U6 snRNA-associated Sm-like protein LSm4
Q8I467	Cofilin/actin-depolymerizing factor homolog 1
Q8I318	EFP domain-containing protein
Q8IK07	Uncharacterized protein
O96265	Small nuclear ribonucleoprotein Sm D2
Q8IC43	Small exported membrane protein 1
O96258	40S ribosomal protein S26
Q8IHU0	60S ribosomal protein L28
O96184	60S ribosomal protein L37a
O97241	Ubiquitin-conjugating enzyme E2, putative
Q8IE05	Trafficking protein particle complex subunit 2,putative
Q8IBD0	Uncharacterized protein
Q8I6T3	Proteasome subunit beta
Q8IM53	Cytochrome c, putative
Q8IIB9	U6 snRNA-associated Sm-like protein LSm1
A0A144A2H0	Aminopeptidase P
Q8IJA5	Transcription elongation factor SPT4, putative
C6KSV0	Histone H3
O97256	Activator of Hsp90 ATPase, putative
Q8I3T9	60S ribosomal protein L2
Q8IKK7	Glyceraldehyde-3-phosphate dehydrogenase
Q8IIJ4	Uncharacterized protein
Q8IBJ9	Mago nashi protein homologue, putative
Q8IJK2	Autophagy-related protein
Q8IIA8	Small nuclear ribonucleoprotein Sm D1
Q8IK02	40S ribosomal protein S20e, putative
Q8IK04	N-terminal acetyltransferase A complex catalytic subunit ARD1, putative
Q8I5C5	Macrophage migration inhibitory factor
Q8IAZ1	Uncharacterized protein
Q8I5V6	U6 snRNA-associated Sm-like protein LSm7, putative
C0H4N9	Uncharacterized protein
Q6ZMA7	Sexual stage-specific protein
P62805	Histone H4
Q8I463	60S ribosomal protein L31
Q8IJT5	Inner membrane complex sub-compartment protein 1
Q8ILB7	Mitochondrial import inner membrane translocase subunit TIM17, putative
C0H4L5	Ribosomal protein L37
Q8IFN5	AP complex subunit sigma
Q8ILN2	Copper transporter, putative
Q8I2N9	CS domain protein, putative
A0A143ZWW5	Ribosome associated membrane protein RAMP4, putative
Q8IDE0	Mitochondrial import inner membrane translocase subunit TIM23, putative
C6KT14	Uncharacterized protein
Q8IFP0	Uncharacterized protein
Q8IER7	Probable DNA-directed RNA polymerase II subunit RPB11
Q8IIX0	60S acidic ribosomal protein P1, putative
Q8IHN5	Uncharacterized protein
Q8I3J4	Ubiquitin-conjugating enzyme E2 N, putative
Q8I3N5	Pre-mRNA-splicing factor BUD31, putative
Q8IIA2	40S ribosomal protein S18, putative
Q8IFN4	BSD-domain protein, putative
Q8IDP4	Thioredoxin 2
C0H574	Uncharacterized protein
Q8IB14	High mobility group protein B2
O97232	1-cys-glutaredoxin-like protein-1
Q8IDB8	HVA22-like protein, putative
Q8IEM3	60S ribosomal protein L24, putative
Q8I4S3	Uncharacterized protein
Q8I488	Parasite-infected erythrocyte surface protein
Q8IM64	Ubiquitin-40S ribosomal protein S27a, putative
C0H4V0	Trafficking protein particle complex subunit 2-like protein, putative
Q8I6V2	Cytochrome c oxidase subunit 2, putative
Q8IJU2	Succinate dehydrogenase subunit 4, putative
O97231	60S ribosomal protein L44
C0H4V6	14-3-3 protein
Q8I3A4	Prefoldin subunit 4
Q8IHP4	Mitochondrial ATP synthase delta subunit,putative
A0A144A372	AP complex subunit sigma
C0H4H3	60S ribosomal protein L39
Q8IKD4	Mitochondrial pyruvate carrier

Table 11. *P. falciparum* proteins identified by LC-MS/MS in the band 3 of Fig. 10.

Accession Number	Protein
Q8IIV2	Histone H4
Q8I467	Cofilin/actin-depolymerizing factor homolog 1
Q8IIV1	Histone H2B
Q8IE09	60S ribosomal protein L23, putative
O77395	40S ribosomal protein S15A, putative
Q8ILX1	Nuclear transport factor 2, putative
Q8ILN8	40S ribosomal protein S25
Q8IJK8	60S ribosomal protein L30e, putative
Q8IHW4	V-type proton ATPase subunit F
C0H529	Small nuclear ribonucleoprotein Sm D3
Q8I5C5	Macrophage migration inhibitory factor
O96184	60S ribosomal protein L37a
Q8II62	60S ribosomal protein L38
Q9NLB0	Membrane magnesium transporter, putative
Q7KQL8	Thioredoxin
Q8IBD0	Uncharacterized protein
Q8IJX8	DNA/RNA-binding protein Alba 3
O96265	Small nuclear ribonucleoprotein Sm D2
Q8IBV7	Histone H2B
Q8IK07	Uncharacterized protein
Q8IDP4	Thioredoxin 2
Q8II72	Parasitophorous vacuolar protein 1
C0H4A3	Rab5-interacting protein, putative
Q8IHY3	Ubiquitin-related modifier 1 homolog
C6KSV0	Histone H3
Q8I488	Parasite-infected erythrocyte surface protein
O77358	Trafficking protein particle complex subunit 4, putative
Q8IM64	Ubiquitin-40S ribosomal protein S27a, putative
O77367	E3 ubiquitin-protein ligase RBX1, putative
A0A143ZWW5	Ribosome associated membrane protein RAMP4, putative
C0H4H3	60S ribosomal protein L39
Q8I607	Ubiquitin-conjugating enzyme E2
C6S3E6	Pterin-4a-carbinolamine dehydratase
O15770	Glutathione reductase
Q8IE87	Uncharacterized protein
Q8I3X2	Mitochondrial import inner membrane translocase subunit TIM16, putative
Q8IJK2	Autophagy-related protein
C0H4E7	SWIB/MDM2 domain-containing protein, putative
Q8IIA8	Small nuclear ribonucleoprotein Sm D1
Q8IC33	Uncharacterized protein
Q8I4Z4	Translation initiation factor SUI1, putative
O97320	Histone H2A
Q8IDR9	40S ribosomal protein S6
Q8I3L8	Mitochondrial import receptor subunit TOM22, putative
Q8IB14	High mobility group protein B2
C0H574	Uncharacterized protein
O96150	DNA-directed RNA polymerase II 16 kDa subunit, putative
Q8I5A5	Mitosis protein dim1, putative
C6KT18	Histone H2A

Graphical Abstract

Several characters were written with a pipette tip by deposition on a PVDF membrane of a suspension of either naïve or *P. falciparum*-infected red blood cells (top photographic image). Upon incubation of the membrane with a solution of a fluorescent DNA aptamer evolved against the latter, only those characters written with parasitized erythrocytes light up (bottom fluorescence image).